2F

PNL-3569
UC-70

Corrosion Resistance of Cast Irons and Titanium Alloys as Reference Engineered Metal Barriers for Use in Basalt Geologic Storage: A Literature Assessment

L. A. Charlot
R. E. Westerman

July 1981

Prepared for
Rockwell International
Rockwell Hanford Operations
under a Related Service Agreement
with the U.S. Department of Energy
under Contract DE-AC06-76RLO 1830

Pacific Northwest Laboratory
Operated for the U.S. Department of Energy
by Battelle Memorial Institute

Battelle

PNL-3569

PACIFIC NORTHWEST LABORATORY
operated by
BATTELLE
for the
UNITED STATES DEPARTMENT OF ENERGY
Under Contract DE-AC06-76RLO 1830

Printed in the United States of America
Available from
National Technical Information Service
United States Department of Commerce
5285 Port Royal Road
Springfield, Virginia 22151

Price: Printed Copy $_____*; Microfiche $3.00

*Pages	NTIS Selling Price
001-025	$4.00
026-050	$4.50
051-075	$5.25
076-100	$6.00
101-125	$6.50
126-150	$7.25
151-175	$8.00
176-200	$9.00
201-225	$9.25
226-250	$9.50
251-275	$10.75
276-300	$11.00

PNL-3569
UC-70

CORROSION RESISTANCE OF CAST IRONS AND TITANIUM ALLOYS AS REFERENCE ENGINEERED METAL BARRIERS FOR USE IN BASALT GEOLOGIC STORAGE: A LITERATURE ASSESSMENT

L. A. Charlot
R. E. Westerman

July 1981

Prepared for
Rockwell International
Rockwell Hanford Operations
under a Related Service Agreement
with the U.S. Department of Energy
under Contract DE-AC06-76RLO 1830

Pacific Northwest Laboratory
Richland, Washington 99352

SUMMARY

A survey and assessment of the literature on the corrosion resistance of cast irons and low-alloy titanium are presented. Selected engineering properties of cast iron and titanium are briefly described; however, the corrosion resistance of cast iron and titanium in aqueous solutions or in soils and their use in a basalt repository are emphasized.

In evaluating the potential use of cast iron and titanium as structural barrier materials for long-lived nuclear waste packages, it is assumed that titanium has the general corrosion resistance to be used in relatively thin cross sections whereas the cost and availability of cast iron allows its use even in very thick cross sections. Based on this assumption, the survey showed that:

- The uniform corrosion of low-alloy titanium in a basalt environment is expected to be extremely low. A linear extrapolation of general corrosion rates with an added corrosion allowance suggests that a 3.2- to 6.4-mm (0.13- to 0.25-in.) thick wall may have a life of 1000 yr. This is a conservative estimate since corrosion rates are expected to be logarithmic (that is, the corrosion rate decreases with time) rather than linear as used in the extrapolation.
- Pitting and crevice corrosion are not likely corrosion modes in basalt ground waters. It is also unlikely that stress corrosion cracking (SCC) will occur in the commercially pure (CP) titanium alloy or in palladiumor molybdenum-alloyed titanium materials.
- Low-alloy cast irons may be used as barrier metals if the environment surrounding the metal keeps the alloy in the passive range. The solubility of the corrosion product and the semipermeable nature of the oxide film allow significant uniform corrosion over long time periods. A linear extrapolation of high-temperature corrosion rates on carbon steels and corrosion rates of cast irons in soils gives an estimated metal penetration of 51 to 64 mm (2 to 2.5 in.) after 1000 yr. A corrosion allowance of 3 to 5 times that suggests that

an acceptable cast iron wall may be from 178 to 305 mm (7 to 12 in.) thick. This is a conservative estimate because it does not take into account the decreasing rate of attack of the metal that is expected as the corrosion product thickness increases.

- Although they cannot be fully assessed, pitting and crevice corrosion should not affect cast iron due to the ground-water chemistry of basalt. Since cast irons are not known to stress crack, SCC or hydrogen stress cracking should not occur in a basalt repository.

CONTENTS

FIGURES

TABLES

INTRODUCTION

The use of metallic barriers between a radioactive nuclear waste form and the host basalt rock is being considered by the Basalt Waste Isolation Project at Rockwell Hanford Operations (RHO) to limit the release of radionuclides to the biosphere. To be effective over an extremely long service life, the metal barriers must be selected to withstand degradation from mechanical (fracture), chemical-mechanical (stress corrosion or corrosion fatigue), and chemical (corrosion) processes. The integrity of the waste package should be assured for approximately 1000 yr;[1] therefore, because of the elevated temperatures expected in a commercial waste repository (to ~523K), this criterion requires substantial extrapolation of current engineering and experience data as well as some insight into the behavior of the candidate barrier materials in a given geologic repository environment.

The purpose of this review is to assess the corrosion resistance of cast irons and titanium alloys in aqueous environments and to estimate the long-term corrosion behavior of each metal in a basalt repository. The review does not consider the actual conceptual design of the metal engineered barrier; but general data on chemical, mechanical, and physical properties of cast iron and titanium alloys are included.

Some assumptions have been made in this report concerning the data that were reviewed; they are summarized below and are expanded in more detail later in the report.

- Because of the good corrosion resistance of titanium in oxidizing environments, it can potentially be used as a metal barrier in thin sections. Low-alloy titanium is already a leading candidate in one Swedish concept for waste storage,[2] and an assessment of its use in a granitic repository has been made.[3]
- Using cast irons as barrier materials offers the benefits of low cost, availability, ease of fabrication, and some favorable mechanical property advantages--that is, immunity to the delayed cracking

problem found in titanium[3] and certain high-alloy steels.[4] Thick sections of cast iron would be used to accommodate the potential metal loss due to corrosion processes.

- The mechanical integrity of the metal barrier should be maintained although some degradation of the metal with subsequent change in physical and mechanical properties could be allowed over the 1000-yr package life.
- The waste package would be stored in a deep basalt formation about 1000 m (3280 ft) deep. The Grande Ronde basalt ground water chemistry has been determined[5] and was considered in this review.

The following literature was searched for relevant data on the corrosion resistance of cast irons and titanium alloys in aqueous environments:

- Metal Abstracts - 1966 to date
- National Aeronautics and Space Adminstration - 1970 to date
- National Technical Information Service - 1970 to date
- Corrosion Abstracts - 1966 to date.

LITERATURE BACKGROUND

A few of the engineering properties that make low-alloy cast irons and titanium alloys attractive candidates as engineered barrier materials are described in this section, and the corrosion resistance of these metals in aqueous environments is discussed.

ENGINEERING PROPERTIES

This document provides background information on the chemical, mechanical, and physical properties of cast iron and low-alloy titanium. Comments have been included on composition, general corrosion resistance, short-term mechanical properties, thermal conductivity, and weldability.

Cast Irons

Specific engineering properties of cast irons are described in detail in various handbooks and other references.[6-11] In this section general statements are presented concerning some of the compositional/chemical, mechanical, and physical properties of cast irons.

Composition/Chemical Properties

Cast iron is basically an iron-carbon alloy with minor additions of silicon, manganese, and phosphorus. The principal constituent found in cast irons that is not found in steels is carbon in the form of graphite, and the form of carbon/graphite in the cast matrix determines the type of iron. Flake graphite occurs in gray irons; carbon bound as cementite (Fe_3C) occurs in white irons; and nodular (spheroidal) graphite occurs in ductile irons. Ferrite in cast irons is essentially a single-phase solid solution of silicon in alpha (body-centered-cubic or BCC) iron. Pearlite consists of alternating lamellae of ferrite and cementite. The composition of typical cast irons is presented in Table 1. The more ductile alloys contain nodular graphite, and the brittle irons contain graphite in flake form.

Generally, ductile and gray irons of the same matrix composition will show similar corrosion behavior. In aqueous environments the graphite in the iron matrix is cathodic and is generally not chemically attacked (corroded).

TABLE 1. Compositional Range for Cast Iron Alloys

Type of Metal	Microstructure: Graphite Form	Microstructure: Matrix	Total Carbon, %	Combined Carbon,[a] %	Si, %	Mn, %	S, %	P, %
White Iron	None	Pearlite + Carbide	1.7 to 3.0	All	0.8 to 1.3	0.4	<0.15	<0.5
Gray Iron	Flake	Pearlite	2.7 to 4.0	<0.9	0.5 to 3.3	0.3 to 1.0	<0.15	<1.4
Nodular[a] Graphite Iron	Nodules	Pearlite or Ferrite	3.3 to 3.9	<0.9	1.6 to 2.5	0.4	<0.01	<0.1
Blackheart Malleable Iron	Nodules	Ferrite	2.0 to 2.7	None	0.8 to 1.2	0.1 to 0.6	<0.15	<0.2
Whiteheart Malleable Iron	Nodules	Pearlite	3.3 to 3.9	0.12	0.1 to 0.8	0.1 to 0.5	<0.4	<0.1

(a) 0 to 1.5% nickel; 0.04 to 0.10% magnesium.

Pearlitic gray irons tend to form better passive films than ferritic irons. A passive film is a corrosion product layer that suppresses or eliminates the corrosion reaction. The cementite phase in a cast iron is electronegative (cathodic) with respect to ferrite, and it would not generally be attacked in an aqueous environment. The presence of cementite in ferritic cast iron could help to suppress general corrosion of the alloy by the process of anodic passivation. Alloying gray irons with phosphorus, copper, or chromium in small quantities improves their corrosion resistance in acidic solutions.

The low-alloy gray irons are resistant to corrosion in dilute alkali solutions. In more concentrated, high-temperature caustic solutions, 3 to 12% chromium is added to impart corrosion resistance. Salts hydrolyzing to acids tend to attack gray irons; salts hydrolyzing to alkalis do not significantly corrode gray irons. In concentrated acid solutions, considerable alloying is done to effect corrosion resistance. For example, Duriron® (17% silicon) and Durachlor® (3.5% molybdenum) resist boiling mineral acids; alloys containing 20 to 35% chromium resist hot alkali and oxidizing acids; and alloys containing >18% nickel are resistant in most aggressive aqueous environments.

High-temperature corrosion (oxidation) of cast irons in air or steam can cause dimensional changes (growth) of the metal as well as scaling. Growth involves both structural changes in the casting and internal oxidation, which generally occur at temperatures above about 723K (450°C) as shown in Table 2. Alloying with chromium, molybdenum, vanadium, or silicon (4 to 8%) normally retards or stops growth by providing protection against internal oxidation.

Mechanical Properties

Tensile strength is frequently used in specifying the grade of a cast iron. As can be seen from Table 3, the tensile strength of gray iron without heat treatment is generally less than 345 MN/m^2 (50,000 psi). When higher strengths are required, chromium, nickel, molybdenum, or copper can be added to the gray iron. Alloying to improve strength may also require special heat

®Trade names of the Duriron Company, Dayton, Ohio.

TABLE 2. Effect of Prolonged Exposure in Air and Superheated Steam on Cast Iron[a]

	Temperature, °C	Duration	Initial Tensile Strength, MN/m^2 (ton/in.^{2})	Gray Iron			Nodular Iron	
				199 (12.9)	239-278 (15.5 to 18.0)	278 (18.0 or more)	Pearlitic 724-755 (46.9-48.9)	Ferritic 434 (28.1)
	400	64 weeks	Growth,[b] %	Nil	Nil	Nil	Nil	Nil
			Scaling, g/dm^2	0.25	0.2	0.19	0.12	0.12
			Loss of strength,[c] %	Nil	Nil	Nil	Nil	Nil
In air	450	64 weeks	Growth, %	0.32 (0.30-0.33)	0.21 (0.05-0.31)	0.13 (0.02-0.26)	0.02-0.03	0.01
			Scaling, g/dm^2	0.45	0.37	0.35	0.23	0.21
			Loss of strength,[c] %	13.4 (-10.3 to -16.5)	7.0 (+7.3 to -13.3)	3.6 (+8.9 to -12.1)	2.5 (0.7-4.3)	7.0
			Loss of hardness,[c] %	16.0 to 19.0	Nil to 26.8	Nil to 30.4	No change	No change
Superheated Steam	427	49 weeks	Growth, %	0.079 (0.25-0.134)	0.0017 (-0.0017 to +0.01)	0.0033 (-0.0017 to +0.01)	-0.01	-0.2
			Scaling, g/dm^2	0.532	0.086	0.052	0.055	0.09
			Loss of strength,[c] %	3.3 gain (-4.0 to +10.7)	3.75 loss (-11.26 to 11.93)	0.63 low (-13.4 to +9.81)	1.3-13.0	0-0.4
			Change of hardness,[c] %	No change	No change	No change	No change	No change

(a) Reference 6, p. 257; Reference 7, p. 793, discusses high-temperature corrosion of cast iron in detail.
(b) Changes of less than 7.0% in tensile strength and 0.02% in growth are unlikely to be significant.
(c) At room temperature after exposure.

TABLE 3. Short-Term Tensile Properties of Cast Irons[a]

Type of Iron	Tensile Strength in Stressed Portion,[b] MN/m^2	Proof Stress (0.1%), MN/m^2	Proportional Limit (0.01%) Deviation from E_o, MN/m^2	Total Plastic Strain at Failure	Young's Modulus, GN/m^2
Gray--Grade 10	154	100	39	0.45 to 0.60	76 to 103
Gray--Grade 12	185	120	51	0.33 to 0.53	83 to 110
Gray--Grade 14	216	141	60	0.22 to 0.47	97 to 120
Gray--Grade 17	263	171 to 193	73	0.38	110 to 131
Gray--Grade 20	309	201	85	0.28	117 to 145
Gray--Grade 23	355	232 to 270	97	0.25	124 to 152
Gray--Grade 26	402	261	111	0.28	124 to 152
Whiteheart Malleable	309 to 371	179 to 196	97 to 198	Elongation %	176
				4 to 8	145 to 179
Blackheart Malleable	278 to 340	170 to 216	130 to 161	6 to 14 min	145 to 186
					172
Pearlitic Malleable	432 to 510	264 to 318	159 to 192	6 to 4 min	145 to 186
Nodular Pearlitic SNG	494 to 726	309 to 386	185 to 232	7 to 2	169 to 176
Nodular Ferritic SNG 27/12	417	261	182	12	169
Nodular Ferritic SNG 24/17	371	224	168	17	169

(a) Reference 6, p. 477; additional detailed mechanical property data can be found in References 8, 9, and 11.

(b) The tensile strength is that obtained in a standard 30-mm (1.2-in.) as-cast test bar of the grade quoted for gray iron. If the stressed portion is of much heavier section, the tensile strength may be much lower and the maximum design stress will be correspondingly lower in accordance with the criteria given.

treatments. Ductile irons are heat treated to develop a specific microstructure with fully annealed irons having a tensile strength of about 414 MN/m^2 (60,000 psi). Generally, tensile strength is greater in pearlitic irons than in ferritic irons.

The endurance limit--that is, the limit to which the material can withstand repeated stressing (fatigue) without fracturing--increases with the tensile strength of the material and decreases with the presence of notches or stress concentration. Gray irons generally have a lower endurance limit than ductile irons, but they are not affected by the presence of notches to the same extent as ductile irons.

Flake graphite inclusions are a source of stress concentration in gray irons because of their lenticular shape. This stress concentration effect reduces the ductility of gray iron to very low levels, and ductility is generally not reported for these materials. The ductile irons, having a spheroidal distribution of graphite in the matrix, do not show the same effect of stress concentration and, therefore, demonstrate ductile behavior. The ductile property of cast irons is evident in their impact resistance: Gray irons normally show low impact resistance whereas ductile irons will show improved toughness.

High-temperature strength is influenced by the stability of the microstructure of the alloy at the use temperature. The ability of iron to maintain a load for long periods of time at elevated temperature is indicated by its creep strength. Although the creep strength of low-alloy cast iron is poor, it can be significantly improved by alloying. The creep strengths of several irons are shown in Figure 1, and the permissible service stress at 623 and 673K is shown in Table 4 for several alloys.

Physical Properties

The damping capacity of a material is a measure of its ability to absorb vibrational energy. The flake graphitic structure of gray irons tends to give better damping properties than the spheroidal graphitic ductile irons. Generally the damping capacity is greater in lower strength irons. Figure 2 schematically compares this property for cast and wrought irons.

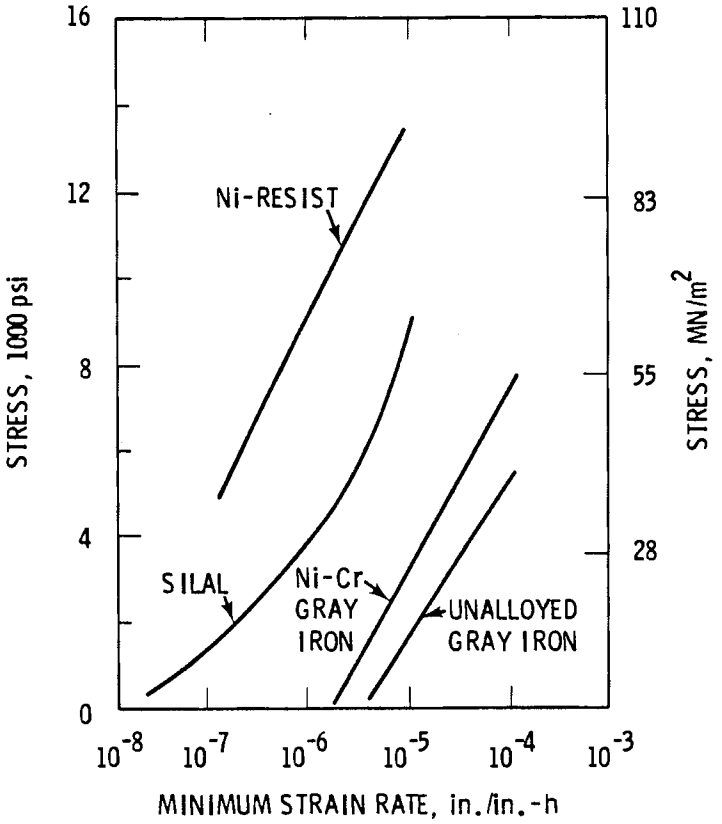

FIGURE 1. Comparative Creep Strengths at 810K for Four Cast Irons (Reference 9)

The thermal conductivity of cast iron is partly dependent on its structure. Pearlite and cementite phases have a low thermal conductivity whereas graphite has a high thermal conductivity. Therefore, gray irons will generally show better thermal conductivity than other types of cast iron. Table 5 lists some values of thermal conductivity for gray iron, nodular iron, and steels at 373 and 673K (100 and 400°C).

Gray, ductile, and malleable cast irons may be fusion welded provided that suitable precautions are taken; these precautions are summarized in a review of cast iron welding by Pearce.[12] In stress-bearing welds, strength and weld integrity are the most important requirements. The main difficulties in fusion welding gray irons (flake graphite structure) are a hard or unmachinable weld zone--due to the redistribution of carbon to the heat-affected zone--and cracking--due to the increased hardness and an inability to accommodate shrink stresses. Ductile (nodular) irons are more readily welded than gray irons due

TABLE 4. Service Stress of Cast Irons at High Temperatures[a]

Type of Iron		Stress at 623K, MN/m^2	Stress at 673K, MN/m^2
Gray--Grade 10 to 12	Short-term tensile	154 to 185	(154 to 185) 170
	Stress to rupture in 100,000 h	93 to 108	62
Gray--Grade 14 to 17	Short-term tensile	216 to 259	216 to 259
	Stress to rupture in 100,000 h	139 to 154	93
	Total creep for 100,000 h, 0.1%	77	28
Gray--Grade 20 to 26	Short-term tensile	309 to 386	293 to 355
	Stress to rupture in 100,000 h	263	124 to 170
Whiteheart Malleable	Stress to rupture in 100,000 h	139 to 216	77 to 154
	Total creep for 100,000 h, 0.2%	31 to 46	15 to 19
Blackheart Malleable	Stress to rupture in 100,000 h	139	77 to 93
	Creep rate for 1000 h, 0.1%	--	83
Pearlitic Malleable	Stress to rupture in 100,000 h	247	154
	Stress to rupture in 100,000 h	309 to 386	201 to 232
Nodular Pearlitic	Short-term tensile	(917) 687	556
	Short-term 0.1% proof	(537) 474	436
	Total creep for 100,000 h, 0.1%	108 to 139	31 to 46
Nodular Ferritic	Stress to rupture in 100,000 h	185 to 216	108 to 124
	Short-term tensile	--	59 to 100
	Total creep for 100,000 h, 0.1%	77 to 93	15 to 23

(a) Reference 6, p. 480.

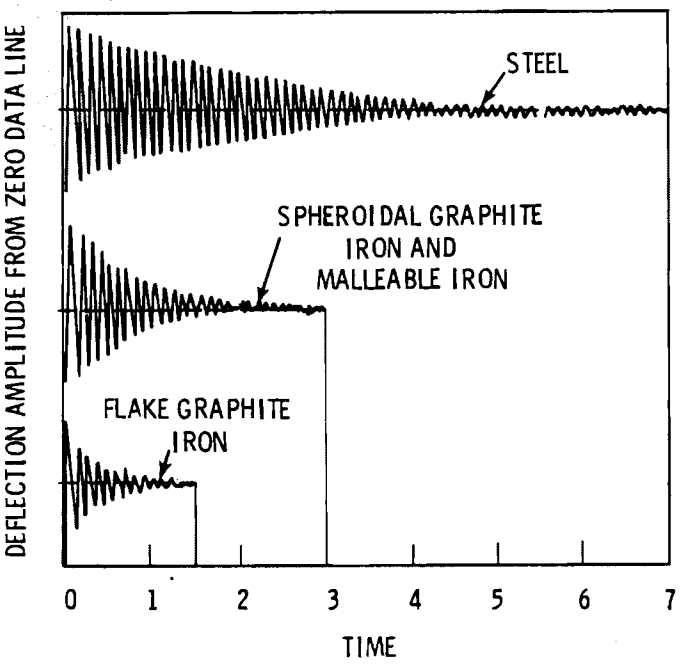

FIGURE 2. Damping Diagram for Steel, Ductile Iron, and Gray Iron (Reference 7, p. 738)

to better ductility and impact resistance, which allows some forgiveness in the shrink stresses developed in the weld zone. However, the redistribution of carbon in these alloys can form martensite or carbides that increase the hardness of the weld zone, thereby increasing the potential for cracking.

Titanium Alloys

As in the preceding section on cast irons, only selected properties of titanium alloys are presented; and they are discussed in general terms. Several references[13,14,15] can supply specific data.

Composition/Chemical Properties

Pure or low-alloy titanium is a hexagonal close-packed (HCP) metal at temperatures to about 1153K. Above this temperature, the HCP alpha phase changes to a BCC beta phase. Alloying titanium with various metals yields a family of stable alloys that can be all alpha, alpha and beta, or all beta. Corrosion resistance and mechanical properties will be affected by the dominant phases in the alloy and its crystallographic texture.

TABLE 5. Thermal Conductivity of Cast Iron and Steel[a]

Material	Mean Temperature, °C	Thermal Conductivity, W/m-°C	Mean Temperature, °C	Thermal Conductivity, W/m-°C
High Carbon	100	59	400	47
High Carbon	100	59	400	46
High Carbon[b]	100	57	400	42
High Carbon	100	56	400	47
Normal Gray:				
Pearlite[c]	100	49	400	40
Annealed Ferritic[c]	100	53	400	44
Low Silicon:				
Perlit	90	57	430	47
	100	65	400	45
White Iron	25	32	--	--
Blackheart Malleable[d]	100	63	400	58
Ferritic	100	49	400	46
Pearlitic	100	44	400	41
Whiteheart Malleable[e]	100	48	400	44
Pure Iron	100	69	400	49
Steel	100	51	400	43
	100	48	400	41
	100	45	400	37

(a) Reference 6, p. 131.
(b) 0.16% chromium; 0.31% molybdenum.
(c) 0.14% chromium.
(d) BS310: 1958 Amendment 1 1962 gives 0.12 to 0.15 cal/cm-s-°C; falls with increasing temperature.
(e) BS309: 1958 Amendment 2 1962 gives 0.11 to 0.15 cal/cm-s-°C; increases with total carbon but decreases with temperature.

Titanium is a reactive metal that can dissolve and retain large amounts of oxygen, hydrogen, and carbon. These elements can cause interstitial hardening, which increases the alloy strength, decreases its ductility, and can lead to embrittlement. However, the corrosion resistance of the metal is extremely good in most environments because of a thin passive oxide film (TiO_2) that forms on the base metal and protects it. Only when the passive film is degraded will accelerated corrosion occur. Titanium does not generally possess good corrosion resistance in low pH reducing environments or in hot concentrated chloride solutions, and pitting or crevice corrosion results in these environments. Under these conditions the commercial alloys normally show a breakdown of the passive film at temperatures greater than 373K, but additions of nickel or palladium to the alloy will increase the breakdown temperature and give improved resistance to both pitting and crevice attack.

The high-temperature oxidation of titanium in air or steam generally follows parabolic kinetics (metal loss proportional to time to the one-half power) with the protective TiO_2 film protecting the metal. Oxidation rates at temperatures less than 673K are generally less than 2.5×10^{-3} mm/yr (0.1 mil/yr).

Mechanical Properties

Titanium alloys have excellent strength-to-weight ratios; but the tensile strength of pure titanium is low, typically less than 241 MN/m^2 (35,000 psi). The tensile strength in commercially pure (CP) alloys is somewhat higher due to iron and oxygen impurities in the metal. Table 6 lists some of the short-term properties of several low-alloy alpha alloys. The increased strength obtained by selective alloying or interstitial hardening causes a reduction in ductility as well as some compromise in other alloy properties. For example, alloying titanium can lead to materials with improved mechanical properties, but they may exhibit an increased susceptibility to stress corrosion cracking (SCC). The Ti-<0.8 Ni alloys were developed to resist pitting corrosion but were found to suffer edge cracking when formed into strip material.[15]

TABLE 6. Short-Term Mechanical Properties of Titanium Alloys[a]

Alloy	Grade	UNS[c]	Composition, %[d]	Condition	Mechanical Properties[b]			
					Yield Strength, MN/m^2 (ksi)	Tensile Strength, MN/m^2 (ksi)	Elongation in 2 in., %	Hardness, HB
Commercially Pure	1	R50250	0.20 Fe; 0.18 O	Annealed	241 (35)	331 (48)	30	120
Commercially Pure	2	R50400	0.30 Fe; 0.25 O	Annealed	345 (50)	434 (63)	28	200
Ti-Pd	7	R52400	0.30 Fe; 0.25 O; 0.12 to 0.25 Pd	Annealed	345 (50)	434 (63)	28	200
Ti-6 Al-4 V	5	R56400	5.5 to 5.6 Al; 0.40 Fe; 0.20 O; 3.5 to 4.5 V	Annealed	924 (134)	993 (144)	14	330
Low-Alloy	12	--	0.2 to 0.4 Mo; 0.6 to 0.9 Ni	Annealed	448 (65)	517 (75)	25	--

(a) Reference 16.
(b) Room temperature properties.
(c) UNS = unified alloy numbering system.
(d) Single values are the maximum composition values.

The creep strength of titanium is reasonably good up to about 873K but decreases rapidly at higher temperatures. The creep strength can be improved by "beta" processing (forging, rolling, or heat treating above the beta transus followed by a solution anneal) or by adding silicon to the alloy. Typical creep strengths for CP alloys are shown in Figure 3.

Physical Properties

The physical properties of CP titanium alloys (or near-alpha alloys) do not differ significantly from one another. The thermal conductivity at 373K is about 21 W/m-°C for titanium compared to 56 W/m-°C for carbon steel.

Machining CP titanium is similar to machining austenitic stainless steel (SS); however, machining becomes more difficult as the metal is more highly alloyed. Welding titanium by gas tungsten or gas metal arc methods will, with some care, give strong, ductile, and corrosion-resistant welds having properties comparable to the parent metal. When iron is present from 0.05 to 0.2 weight percent (wt%), the ductility and forming characteristics of the weld are improved; however, the increased iron content decreases the corrosion resistance of the weld when it is exposed to hot acidic solutions.[15]

UNIFORM CORROSION

Aqueous corrosion is an electrochemical process where oxidation occurs at the anode of an electrochemical cell and reduction occurs at the cathode. For example:

$$Fe \longrightarrow Fe^{++} + 2e^{-} \qquad \text{(anodic reaction)}$$
$$2H^{+} + 2e^{-} \longrightarrow H_2 \text{ or} \qquad \text{(cathodic reaction)}$$
$$O_2 + 2H_2O + 4e^{-} \longrightarrow 4OH^{-} \qquad \text{(cathodic reaction).}$$

For iron the Fe^{++} ion is not stable in solution and will react with oxygen or water to form magnetite (Fe_3O_4), hematite (Fe_2O_3), or other stable, soluble ionic species. The equilibrium between the metal and its corrosion products in an aqueous media can then be thermodynamically described by potential-pH diagrams such as those shown in Figure 4 for iron and titanium. The Pourbaix diagrams show regions where chemical stability can be expected. Standard texts[17,18,19] describe the construction, application, and limitation of the

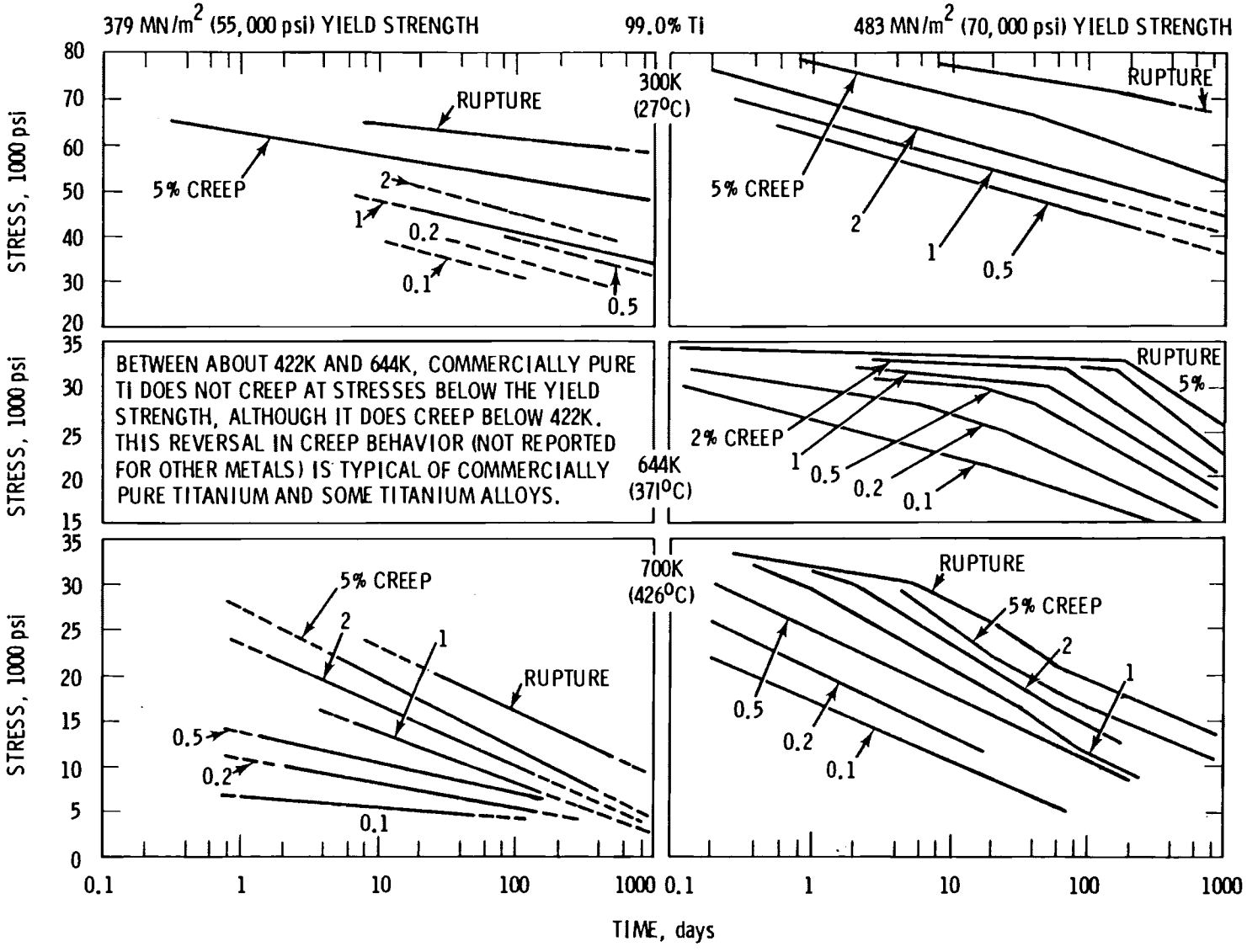

FIGURE 3. Creep Strengths of Commercially Pure Titanium (Reference 8, p. 537)

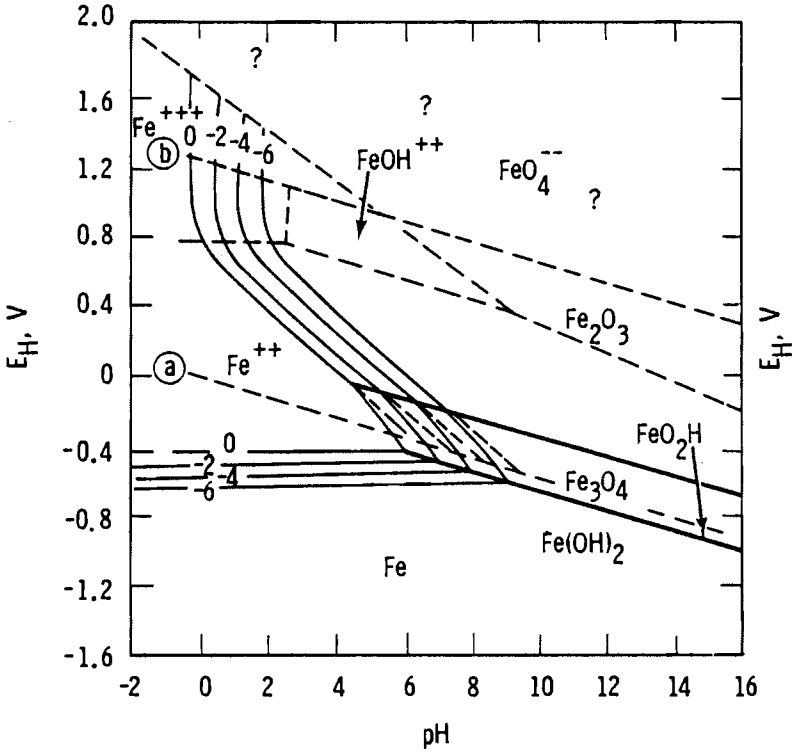

a) $Fe-H_2O$

b) $Fe-H_2O$, Showing Areas of Passivation

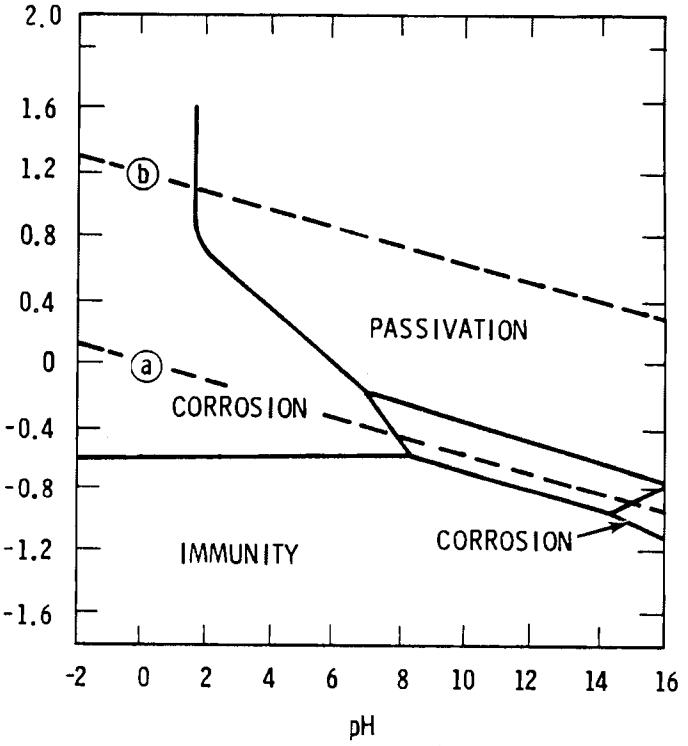

FIGURE 4. Potential-pH Diagrams at 298K (25°C) for $Fe-H_2O$ (a) (Reference 17, p. 17), $Fe-H_2O$ Showing Areas of Passivation (b) (Reference 17, p. 18), and $Ti-H_2O$ (c) (Reference 3). Parallel dashed lines refer to the stability of water; line a is the reduction to hydrogen; and line b is the oxidation to oxygen.

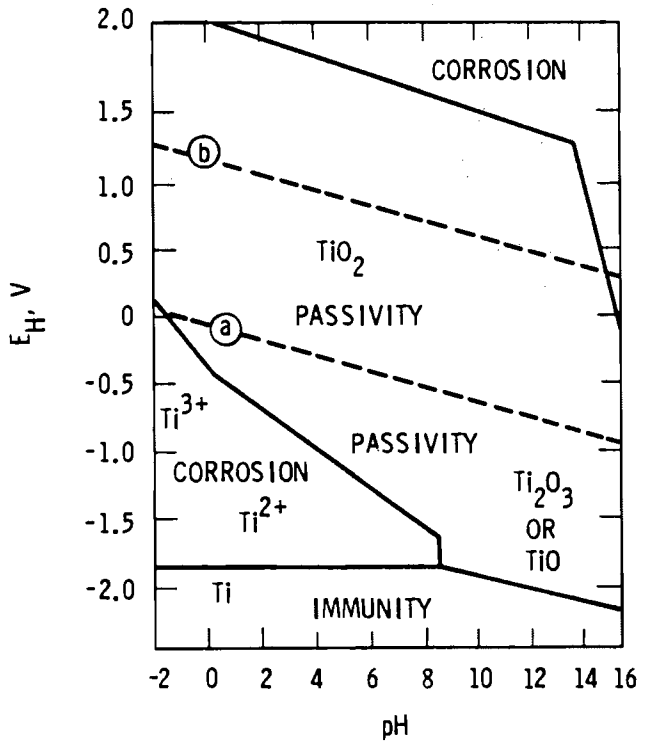

c) Ti-H_2O

FIGURE 4. (contd)

diagrams. Several diagrams have been included in this paper to describe the corrosion process in terms of thermodynamic regions of active corrosion, passivation, and immunity.

Uniform metal penetration by corrosion processes can be severe in low-alloy carbon steels or cast irons, but it may not be a primary metal degradation phenomena in titanium alloys. The rate of uniform corrosion is expressed in terms of metal penetration--mils per year (mpy)--or weight change--mg/dm^2/day (mdd).

Cast Irons

The uniform corrosion of cast irons in an aqueous system is comparable to the corrosion of iron or low-alloy carbon steels except that the graphite content in the cast irons will change the corrosion rate due to the formation of a graphite-rust layer between the metal and the environment. The areas of active corrosion or passivation shown in Figure 4 hold for the cast irons as

for any low-alloy carbon steel. Much of the literature that was reviewed considers the use of cast iron in pipeline service. These corrosion data are relevant to soil (underground) corrosion but are limited in that the effect of temperature on the uniform corrosion process is generally not considered. Cast irons are used in low-temperature boiler service; and data from this use will allow some insight into the effect of temperature, particularly when compared to low-alloy carbon steel corrosion data. A problem with using corrosion data from boiler service is that the chemistry of the high-temperature water is generally controlled to keep the carbon steels within the passive region of the Pourbaix diagram.

Soil (Underground) Corrosion

The corrosion resistance of cast iron pipelines can be attributed to: 1) the heavy wall of the pipe, 2) the graphite and in some gray irons a phosphorus intermetallic phase that helps to form a corrosion product coating, and 3) the use of insulated short section pipes in actual service. Gray irons that have a flake graphitic structure tend to lose strength and become susceptible to mechanical failure after graphitization[a] of the pipe takes place. Ductile cast iron generally has twice the initial strength of gray iron for a given thickness and shows less strength loss due to uniform or localized corrosion.[20]

The major parameters dictating soil corrosion of metals are pH, electrolyte concentration, moisture content, and soil resistivity. The most corrosive soils are those having large concentrations of soluble salts such as sulfates, chlorides, and bicarbonates; low resistivity; and either a very acid or very alkaline pH.[21,22] The National Bureau of Standards (NBS) has determined the corrosion behavior of ferrous pipe materials buried in soil environments over a 30-yr period.[23,24] One of their basic conclusions--that ductile cast iron and carbon steel "may corrode at nearly the same rate when buried in some soil environments...,"[23]--has been subject to criticism[20,25] because of the analysis of the pitting attack and the choice of soil (most of the test beds

(a) Graphitization is a process of selective corrosion of gray irons where the iron or corrosion products are lost from the structure leaving the graphite in place.

consisted of very aggressive media). Whether the analysis is correct or not does not change the observation that ferrous metal test pipes failed by a localized corrosion process and not by uniform corrosion.[21] These results will be described in a later section on pitting corrosion.

In Table 7 the weight loss of carbon steel, malleable iron, and gray iron is shown for several soils of differing resistivity. It is difficult to establish a "typical" soil corrosion rate from these data since the maximum change in rate is about a factor of 16 for malleable iron in the various soils. For a given soil, the change is a factor of about 10 between gray and malleable irons. In underground service gray irons are generally considered to have better corrosion resistance than either ductile iron or carbon steels,[26] but ductile irons have a greater resistance to localized attack than gray irons.[27]

Figure 5 shows that there is little difference in the corrosion behavior of gray cast irons fabricated by sand casting or spin casting, although the spun cast irons consistently show slightly lower weight loss. The sand cast pipe had a pearlitic/flake graphite structure while the spun cast pipe had a ferritic/fine flake graphite structure. If the rates shown in Figure 5 are compared to those in Table 7, one again sees the problem in arriving at a typical corrosion rate for cast irons in soil environments.

TABLE 7. Comparative Corrosion Rates of Ferrous Metals in Soil After 10-yr Burial[a]

	Corrosion Rates, mg/dm^2-day					
	Soil Resistivity, Ω/cm					
Metal	60	263	408	1270	11,400	13,700
Steel	6.8	15.8	14.1	9.7	3.2	6.2
Malleable Iron	16.8	14.0	11.7	0.9	0.9	5.9
Gray Iron	8.9	14.0	26.2	12.6	3.7	9.4

(a) Reference 6, p. 320.

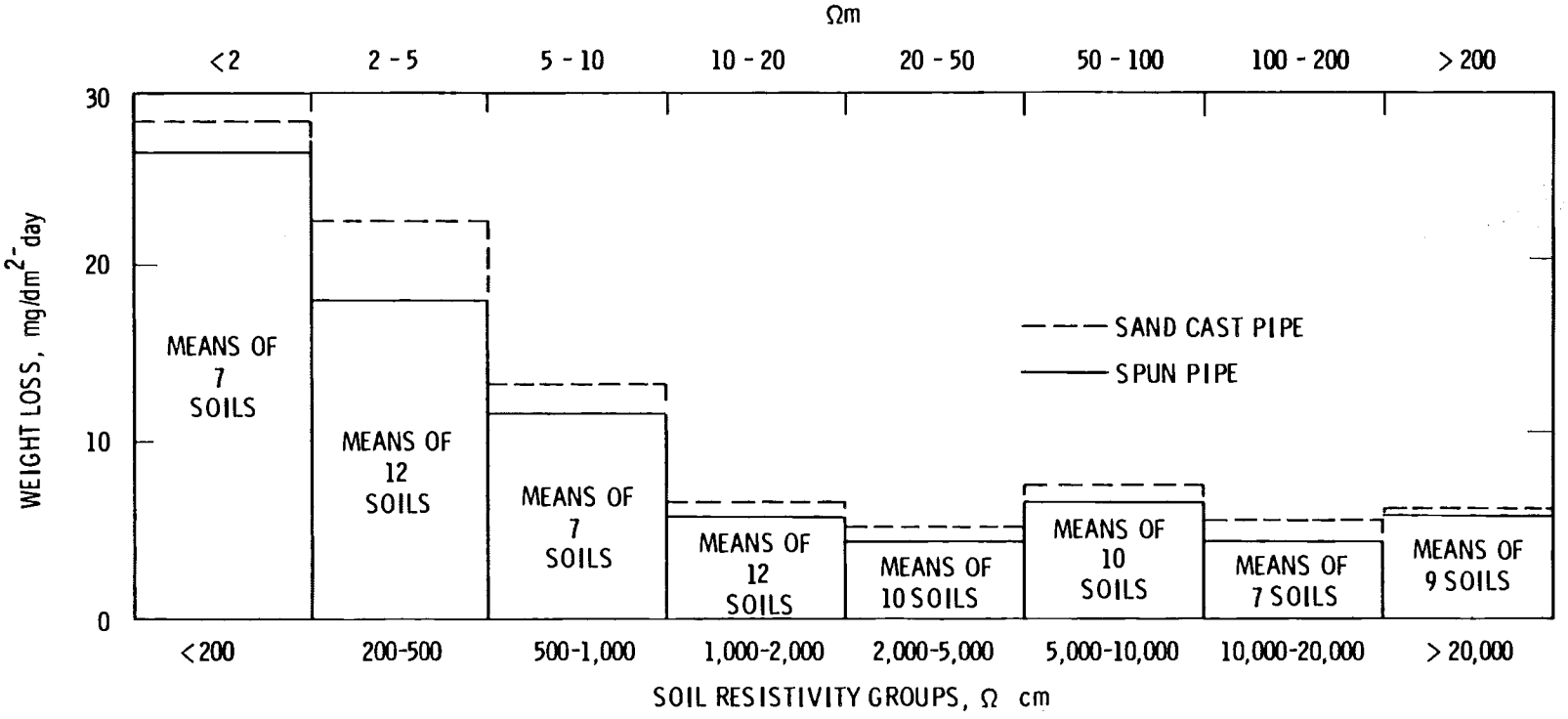

FIGURE 5. Corrosion of Gray Iron in Soils of Differing Resistivity (Reference 22)

Natural and Sea-Water Corrosion

Pure water does react slowly with cast irons to evolve hydrogen and form generally protective, passive oxide surface films. Dissolved salts in neutral waters can act to either accelerate general corrosion or to protect cast irons by passivation. Chromates, nitrites, nitrates, and permanganates are all oxidizing salts that tend to passivate metals in near-neutral pH solutions; however, these same salts will tend to accelerate uniform corrosion in acid pH solutions.[17] Well-aerated, neutral solutions of chloride and sulfate salts act to accelerate both uniform and localized corrosion of cast irons with the average uniform corrosion rate ranging from 1 to 5 mpy in static or quiet waters.[12]

The corrosion rates of several cast alloys in sea water are compared in Table 8. In fresh water the deposition of calcium carbonate on cast irons can act as a physical barrier between the metal and the environment. The formation of the carbonate layer is dependent on the excess carbon dioxide in the waters. Generally so-called hard waters show a tendency to deposit the carbonate and in doing so are not particularly corrosive to cast irons.[28]

Boiler Water Corrosion

In high-temperature (above 473K) water systems, cast iron or cast steel is primarily used for specialized process equipment such as erosion-resistant impellers or large pump housings. Consequently, corrosion data are limited and usually specific to a particular phenomena such as cavitation-erosion. At lower temperatures (323 to 373K) cast irons have been used in radiators or central heating boilers.

McEnaney and Smith[29] have studied the corrosion of a gray cast iron in neutral pH (6.0 to 7.7), low-oxygen (<1.0-ppm) water containing about 70-ppm chloride and 30-ppm sulfate ion. The cast iron formed a passive film that grew by a parabolic rate; the overall reaction was: $3Fe + 4H_2O \longrightarrow Fe_3O_4 + H_2$.

Figure 6 is an Arrhenius plot of the corrosion of carbon steel in high-temperature alkaline solutions and includes McEnaney's cast iron corrosion rate data. The graph indicates that the corrosion mechanism over the temperature

TABLE 8. Corrosion Rates for Cast Iron Exposed in Sea Water in Various Tests[a]

Metal	Corrosion Rates, mg/dm^2-day[b]				
	Emsworth, U.K., for 2 yr	Cuxhaven, Germany for 6 mo	Laboratory, for 380 days	Laboratory,[c] for 220 days	Harbor Island, USA, for 3 yr
Steel	--	44	24	18	--
Gray Iron	12	17	17	6	813 μm/yr[d]
White Iron	--	--	--	9	--
Malleable Iron	16	--	--	9	--
Pearlitic Nodular Graphite Iron	--	10	--	14	279 μm/yr[d]
Ferritic Nodular Graphite Iron	--	21	16	5	--

(a) Reference 6, p. 316.
(b) Except where noted.
(c) Artificial sea water.
(d) Rate of pitting = 100 mg/dm^2-day = 0.020 in./yr = 508 μm/yr.

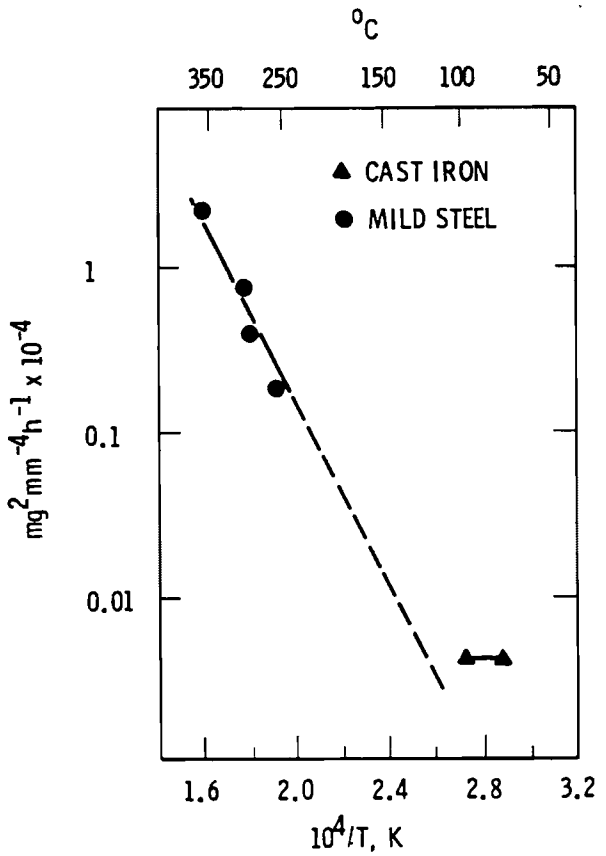

FIGURE 6. Comparison of the Parabolic Rate Constants for Cast Iron (Reference 29) and Mild Steel (Reference 30)

range is essentially the same for both metals. In a separate study,[30] the protective film on the cast iron was identified as a combination of green rust[a] and Fe_3O_4.

(a) Green rust is an intermediate oxide between iron and magnetite that can be schematically shown by:

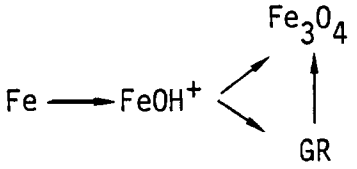

where GR = green rust.

Oxygen was shown to change the composition of the passive film during the corrosion of iron at 323K. In the deoxygenated system (<0.06-ppm O) only green rust and Fe_3O_4 formed, giving the corrosion rate shown in Figure 6. At higher oxygen levels the film was composed of a combination of iron oxides (see Table 9). The corresponding rate data for the film growth were found to be proportional to the oxygen content: about 2.0 to 2.6 x 10^{-8} g/cm^2-s per ppm O_2. An oxygen dependence for mild steel in 298K 6.4 pH water is 1.9 x 10^{-8} g/cm^2-s per ppm O_2.[32]

Comparisons of film composition, corrosion rate, and influence of oxygen on the uniform corrosion of cast iron and mild or low-alloy steel allow some confidence in applying the high-temperature aqueous corrosion data for low-alloy steels (where there are considerable data) to the corrosion of cast irons (where there are relatively limited data). In high-temperature water (473 to 573K) irons tend to form only two stable oxides--Fe_2O_3 and Fe_3O_4--according to the Pourbaix diagram for iron-water at 473K,[33] see Figure 7. It can readily be seen that as the oxidant level in the water is increased, the electrochemical potential also increases in a direction favoring passivation

TABLE 9. Composition of Scales Formed on Cast Iron After 6 h at 323K as a Function of Oxygen Concentration[a]

Oxygen Concentration, ppm	Green Rust	Fe_3O_4	γ-FeOOH	α-FeOOH
0.10[b]	+	+		
0.60	+	+		
1.10	+	+	+	
1.65	+	+	+	
2.00	+	+	+	
3.00	+	+	+	trace
3.95	+	+	+	trace

(a) Reference 31.
(b) Scale formed after 78 h.

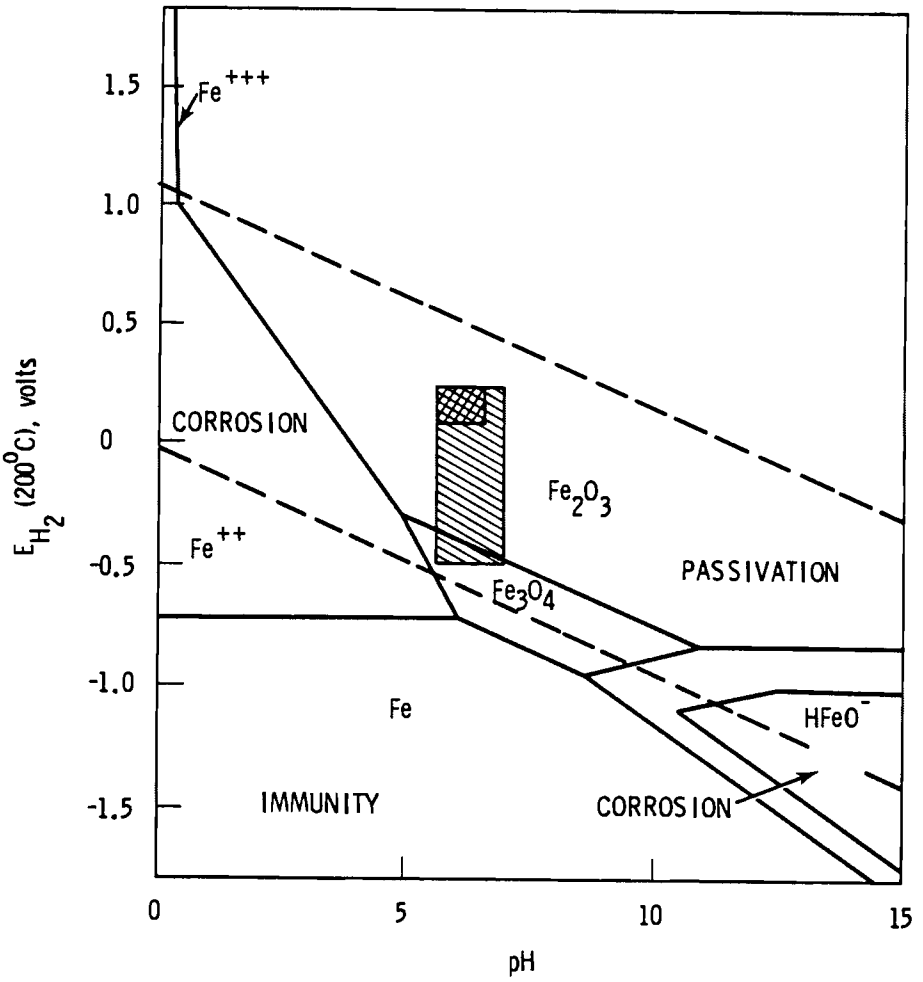

FIGURE 7. Potential-pH Diagram for Fe-H_2O at 473K (200°C) (Reference 33). Shaded area is potential region for oxygenated neutral water; cross-hatched area is potential region for hydrogen peroxide addition to neutral waters (Reference 34).

of iron by Fe_2O_3. "Neutral water conditioning" is a method where either gaseous oxygen or hydrogen peroxide is added to neutral high-purity boiler water to help protect carbon steels. Table 10 shows the corrosion behavior of carbon steel in flowing high-temperature water at various oxygen levels. The temperature effect is not consistent with an Arrhenius relation for any oxygen level, and the greater corrosion resistance is at higher oxygen levels. Instead of raising the anodic potential to protect the iron, passivation can be maintained in deoxygenated solutions if the pH is maintained between 7 and 12. In the

TABLE 10. Corrosion Rate Behavior of Carbon Steel in Neutral pH Feedwater Flow at 1.8 m/s[a]

System and Temperature, °C	Corrosion Rate, mg/dm²-mo				
	Oxygen Content, ppb				
	<1	3	15 to 30	200[b]	2000[b]
Simulated					
38	154	116	18.5	1.2	
66	291	188	16.9	0.1	
93	322	284	16.5	2.2	
121	173	284	8.5	4.3	
149	240	208	4.4	3.3	
177	224	207	0.1	2.9	
204	132	164	8.4	3.8	
In-Plant					
49	--	--	30.5	--	--
82	--	--	--	--	5.0
132	--	--	8.9	--	--

(a) Reference 34.
(b) With stoichiometric ($=O_2/8$) hydrogen.

former case, passivation occurs due to formation of Fe_2O_3 film; but in the latter case, passivation occurs due to Fe_3O_4 or a duplex layer of Fe_2O_3 depending on the oxygen content in the water.[34]

Pearl and Wozadlo[35] found that the corrosion rates of carbon steels were initially fast but decreased to a linear growth rate of about 4 mg/dm²-mo in 558K high-purity neutral water containing about 20-ppm O. As the oxygen content was lowered to 0.2 to 1.2 ppm, the passive film still gave protection but the growth rate was about the same. Mild steels exposed to high-temperature alkaline solutions were found to corrode at rates considerably higher than Pearl's data.[36] Figure 8 shows the effect of sodium hydroxide concentration on the corrosion rate of mild steel and the temperature dependence of the corrosion reaction. The corrosion of the steel in high pH, alkaline solutions is near the active corrosion area shown in Figure 7.

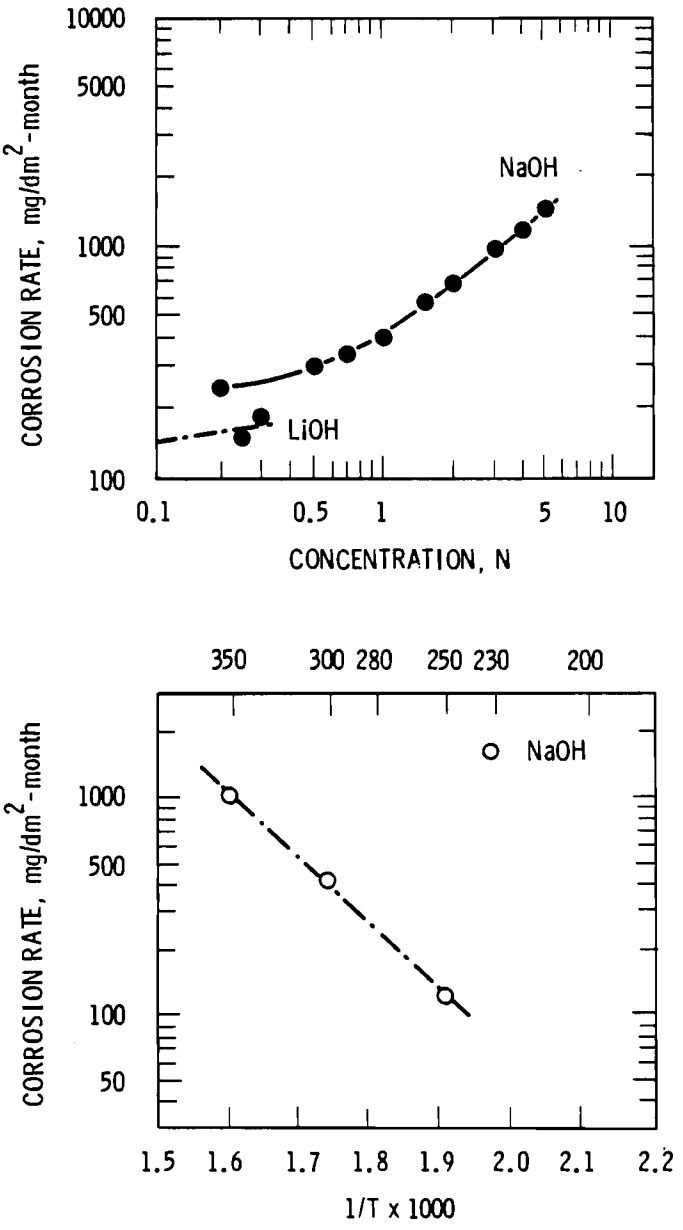

FIGURE 8. Corrosion Rates of Mild Steel as a Function of Concentration of NaOH and Temperature

The high-temperature aqueous corrosion of carbon steels has been summarized in a number of papers.[17,37,38] The uniform corrosion of a carbon steel depends on the stability of the passive layer and the relative solubility of the iron oxide film. If the chemistry of the environment can be maintained to give a pH and potential that puts the metal in the passive area of the Pourbaix

diagram, then the corrosion of the metal will follow parabolic or slow linear kinetics. If the high-temperature chemistry changes to give oxygen concentration cells, highly acidic or highly basic conditions, or chloride and sulfate impurities in the vicinity of the metal, the probability for pitting or other nonuniform attack increases. In oxygenated systems the purity of the water becomes important in limiting localized corrosion so that in some cases it is better to remove the oxygen and increase the pH rather than remove the impurities.

Titanium Alloys

The corrosion of titanium in aqueous systems occurs by the reaction of water with metal to form rutile and hydrogen:

$$Ti + 2H_2O = TiO_2 + 2H_2 \qquad (1)$$

The titanium oxide forms on the metal surface and is extremely protective, accounting for the broad region of corrosion passivity shown in the Pourbaix diagram in Figure 4. The growth of the oxide film on titanium follows a parabolic rate law up to about 773K.[39] In high-temperature (573 to 623K) deionized water, Cox[40] found only a 0.3- to 0.5-μm thick oxide film on titanium after several hundred days of exposure. In simulated pressurized water reactor (PWR) environments (573 to 613K, 0.01-ppm O_2, alkaline pH), the weight change on titanium samples exposed 2500 h was only 10^{-2} mdd or about 3×10^{-3} mpy.[41]

The very effective passive layer on titanium can be lost in low pH reducing solutions that cause general dissolution of the metal [to the soluble Ti(III) ion[42]] or in halide or sulfate solutions that promote localized film breakdown. The film may be very protective, however, in environments of relatively high chloride content and at moderate temperatures. The NBS(43) included CP titanium in their field tests of the soil corrosion of metals and found no corrosion of titanium that had been buried for 8 yr, even in clay soils containing 3500-ppm Cl ion at pH 4. In corrosion tests in 3 wt% NaCl aerated and deaerated solutions, the metal penetration amounted to only

0.01 mpy at 333K and 0.12 mpy at 473K.[44] In more concentrated chloride solutions, the corrosion rates increased depending on the oxygen content and the titanium alloy. Table 11 is taken from the recent literature and shows uniform corrosion rates for CP Ti, Ti-grade 12, and Ti-Pd alloys.

PITTING AND CREVICE CORROSION

Both pitting and crevice corrosion are localized forms of attack to metals that are generally accelerated by chemical and electrochemical processes differing from the bulk environment-metal interactions. Crevice attack is found in areas where the access of the bulk environment is limited, such as under bolts or between mated flanges. Pitting occurs at the free surface, but it is initiated by some artifact in the metal or some change in the local environment. In both phenomena the chemistry of the pit or crevice area becomes acidic, and the corrosion process is generally accelerated. Pitting requires

TABLE 11. Effect of Oxygen and Temperature on the Uniform Corrosion Rate of Titanium Alloys[a]

Effect of Temperature in Deoxygenated Brine

	Corrosion Rate, μm/yr		
Alloy	343K (70°C)	423K (150°C)	523K (250°C)
Ti-50A	<0.06	2.6	14
Ti-Grade 12	<0.07	0.9	3.2
Ti-Pd	<0.09	0.3	2.4

Effect of Dissolved Oxygen at 523K (250°C)

	Corrosion Rate, μm/yr			
	Sea Water		Brine A	
Alloy	0-ppm O_2	500-ppm O_2	0-ppm O_2	450-ppm O_2
Ti-50A	11.7	16.2	14	3200
Ti-Grade 12	1.10	0.60	3.2	1.8
Ti-Pd	1.14	0.62	2.4	0.4

(a) Reference 45.

higher anodic potentials for initiation and will have high current densities compared with crevice attack. The localized attack of cast irons and titanium alloys under pitting and crevice corrosion is discussed in the following sections.

Cast Irons

There are many examples in the literature that show that the failure of ferrous pipe is not by uniform corrosion but by a combination of localized attack (generally in the form of pits) and a mechanical overload. The NBS has examined cases of underground pipe failures where, for example:

- A 0.15-m (6-in.) diameter cast pipe suffered mechanical overload failure because nonuniform corrosion penetrated about 10% of the pipe cross section. Examination of the pipe showed that the ferrite phase in a pearlite/ferritic matrix was preferentially corroded.[46]
- A 0.10-m (4-in.) diameter gray cast iron gas main failed mechanically due to a crack starting at the bottom surface where graphitization consumed about 25% of the wall.[47]
- A 0.25-m (10-in.) diameter gray cast iron pipe gas main failed because of a combination of graphitization, preferential ferrite attack, and poor initial microstructure.[48]

Localized corrosion leading to failure of ferrous metal in the unstressed state requires that several electrochemical conditions be met prior to the accelerated corrosion process. The passive oxide film is generally lost so that a pit can be initiated at the free metal surface or that the attack can be accelerated in creviced areas. Halides, particularly chloride, in solution are well known for their deleterious effect on the passive film[49,50] and subsequent localized attack. In Figure 9--the Pourbaix diagram for iron in a chloride solution--the conditions for "imperfect" passivity of the oxide are shown at point 2 (pH = 8), which leads to pitting and at point 1 (pH = 8), where crevice corrosion can occur. The high anodic potential required for pitting attack compared to the crevice attack is shown in this figure.

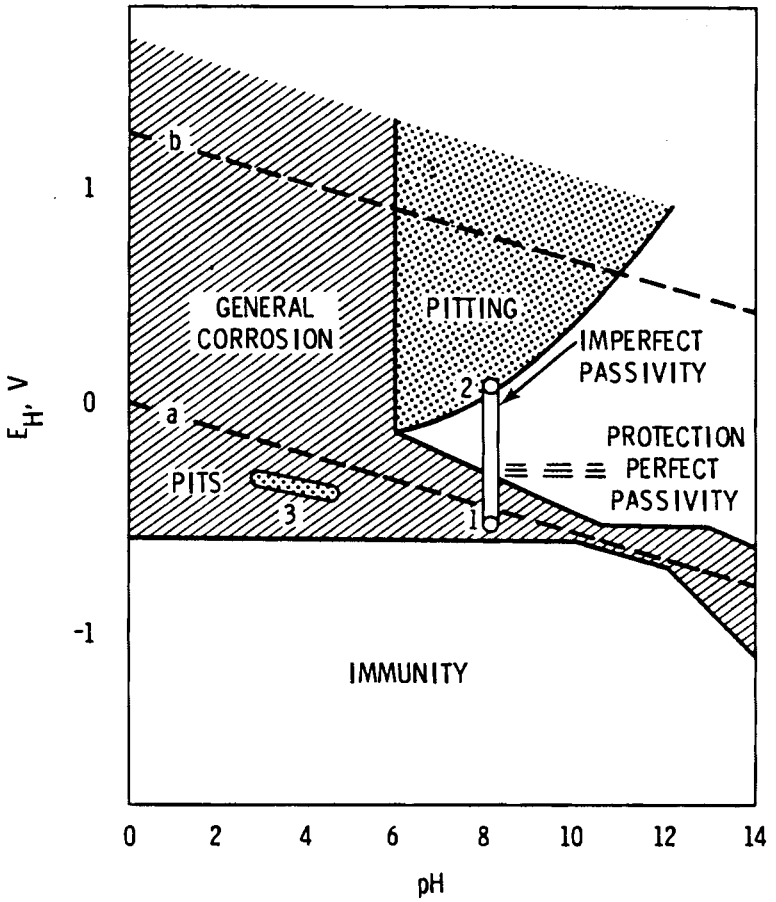

FIGURE 9. Electrode Potentials of Iron in a Solution of pH 8, 355-ppm Cl^-. Line 1: oxygen-free solution and general corrosion; line 2: oxygen, nonpolarized, and pitting; line 3: active pitting and crevice attack. (See Reference 53).

Once pitting is initiated, the potential decreases and the rate or extent of attack becomes dependent on the chemistry in the pit. The chemistry of pitting corrosion in carbon steel has been discussed by Wranglen.[51,52] The corroding metal in the pit and in the creviced area is in an acidic environment compared with the bulk solution. Figure 10 schematically shows the many reactions that can occur in ferrous metals.

In addition to the chemistry of the environment acting on the localized corrosion process, the microstructure of the ferrous alloy also becomes important in dictating the initial local cathodic/anodic reactions on the metal surface. For example, the graphite in cast irons will be cathodic to ferrite. The effect of the pearlite-ferrite-graphite structures on pitting attack has

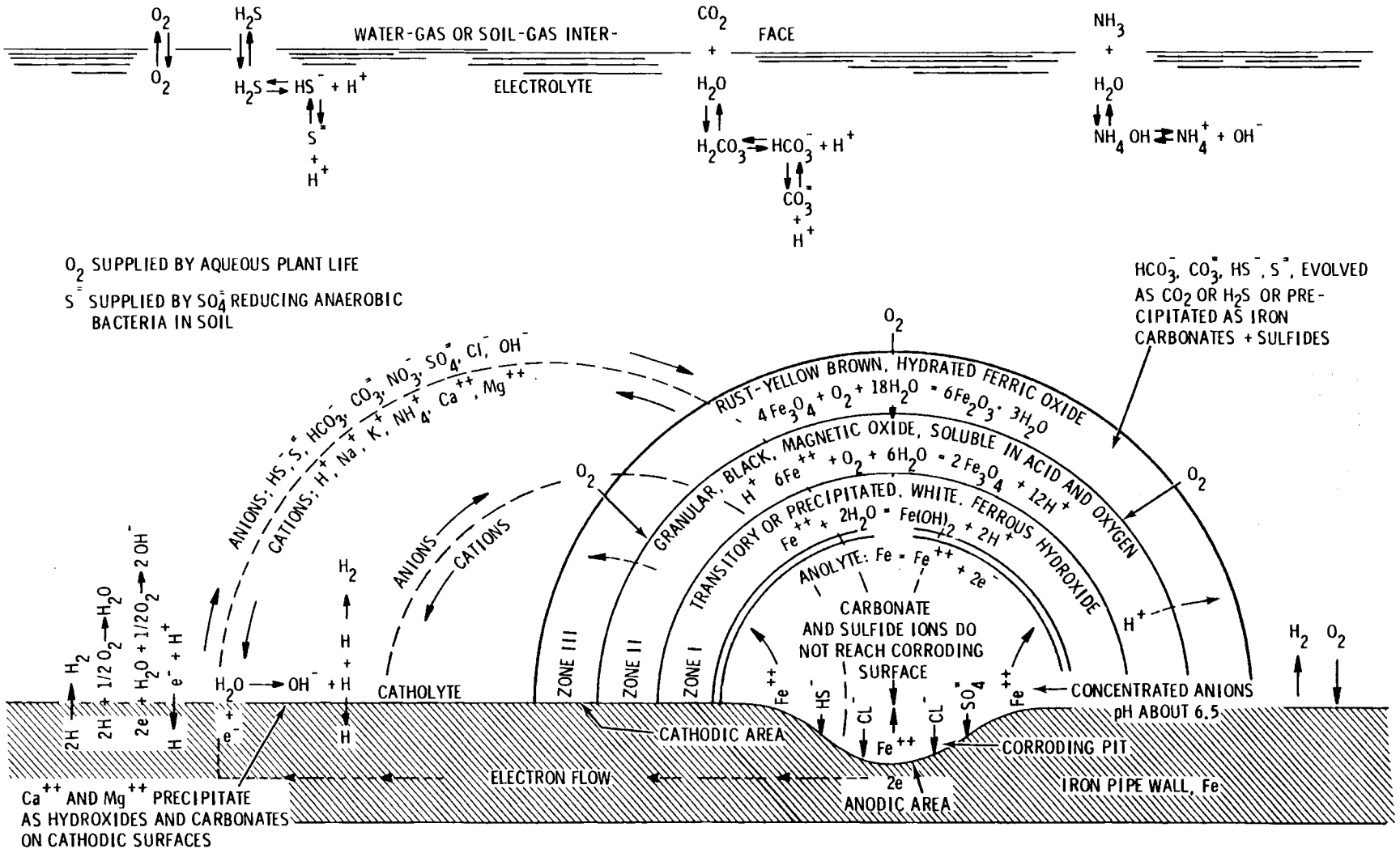

FIGURE 10. Schematic of Underground Corrosion Process (Reference 21)

not been studied; however, there are failure cases of cast irons[47,48] and cast steels[52] that have been attributed to preferential attack of ferrite. Some studies on carbon steels[53] have shown that structural changes in pearlite lead to preferential attack of carbide or ferrite depending on pH, anodic potential, and the anions present in solution. Wranglen[52] compared the pitting corrosion of conventional (ingot) cast steel to a "concast" (continuously cast) steel and found that active sulfide inclusions (MnS) in the concast steel accounted for an increase in pitting in these steels. When the sulfides are made inactive by heat treating to form (MnFe)S or tied to calcium in the alloy, there appears to be no difference in the pitting resistance of ingot or concast steel.

Pitting or crevice attack can be stopped by "healing" the pit and returning the metal to a passive state.[54] The dependence of localized corrosion on pit/crevice chemistry and bulk solution chemistry as well as on the microstructural features of the metal makes the prediction and extrapolation of localized corrosion very difficult.

From the very extensive data gathered by the NBS, an expression for the maximum pit depth (P) in mils has been empirically developed for ferrous metals in soils of different resistivity and pH:

$$P = K_n K_a (10 - pH)^n (\theta/\rho)^n A^a \qquad (2)$$

where ρ = soil resistivity in ohm-cm

θ = time in years

A = exposed surface area in ft^2

K_a, a = material-dependent factors

n = 1/6, 1/3, 1/2, or 2/3 for soils that are well aerated, fairly well aerated, poorly aerated, or poorly aerated with soluble corrosion products, respectively

K_n = 170, 222, or 355 for soils that are well aerated, fairly well aerated, or poorly aerated, respectively.

The material parameters for wrought iron, steel, and cast iron are given in Table 12, which essentially shows that cast iron pipe suffers greater pit depth for larger exposed areas than steel pipe but that as the areas become smaller the maximum pit depth becomes comparable.

Even with the formalism attempted in Equation (2), determination of the material parameter is subject to considerable scatter so that no generalizations should be made. It seems to be a more common approach to quantify pitting corrosion statistically, expressing maximum pit depth as a function of the probability of finding any given pit depth on a certain area of metal.[55] Comparisons such as those shown in Table 13 are then considered more reliable; however, even this approach can lead to questionable conclusions. Crews[25] suggests that the service life of ductile iron can be 11 times greater than steel pipe in representative soils. Fuller[20] shows (see Figure 11) the relation between gray and ductile iron. Although ductile pipe is more resistant to pitting than gray pipe, the resistance is not necessarily improved by a factor of 11.

If uniform corrosion protection is lost, then localized forms of chemical attack can degrade the metal. The loss of passivity of the oxide on iron occurs in halide solutions and has been extensively studied.[49,50] Generally passive film breakdown does not occur until the chloride concentration reaches about 10^{-3} M (37 ppm).[50] The passive films formed in high-temperature waters apparently do not suffer breakdown at this level since neither McEnaney[29,31] or Mann[30] reported significant pitting on ferrous alloys in chloride-containing environments.

TABLE 12. Values of the Material Parameters Used in Equation (2)

Parameter	Wrought Iron	Steel	Cast Iron
K_a	1.00	1.06	1.40
a	0.13	0.16	0.22

TABLE 13. Long-Term Soil Corrosion Comparison for 6-in. Pipe[a]

Soil	Exposure, yr	Mean Weight Loss, mdd[b]		Mean Maximum Pitting, mpy[c]		Mean Loss in Burst Strength, %	
		Ductile Iron	Gray Iron	Ductile Iron	Gray Iron	Ductile Iron	Gray Iron
Cinders	3.7	12.2	10.6	35	35	<10	20
	5.9	15.9	16.0	32	32	<10	30
	7.9	12.5	13.8	27	28	<10	31
	9.4	10.6	11.7	18	22	<10	27
	13.5	9.3	11.3	11	20	<15	40
Alkali	3.7	7.2	5.4	22	16	<10	10
	6.0	4.3	3.2	13	10	<10	10
	8.0	3.2	2.3	10	14	<10	24
	9.9	2.3	1.6	10	9	<15	42
	12.0	2.6	2.2	8	10	<15	41
	14.0	2.4	1.9	9	13	<9	39

Type of Iron	Element, %					
	Carbon	Silicon	Sulfur	Manganese	Phosphorus	Magnesium
Ductile	3.40	2.40	0.01	0.30	0.05	0.04
Gray	3.40	1.50	0.08	0.50	0.60	--

(a) Reference 11.
(b) mdd = mg/dm^2-day.
(c) mpy = mils per year.

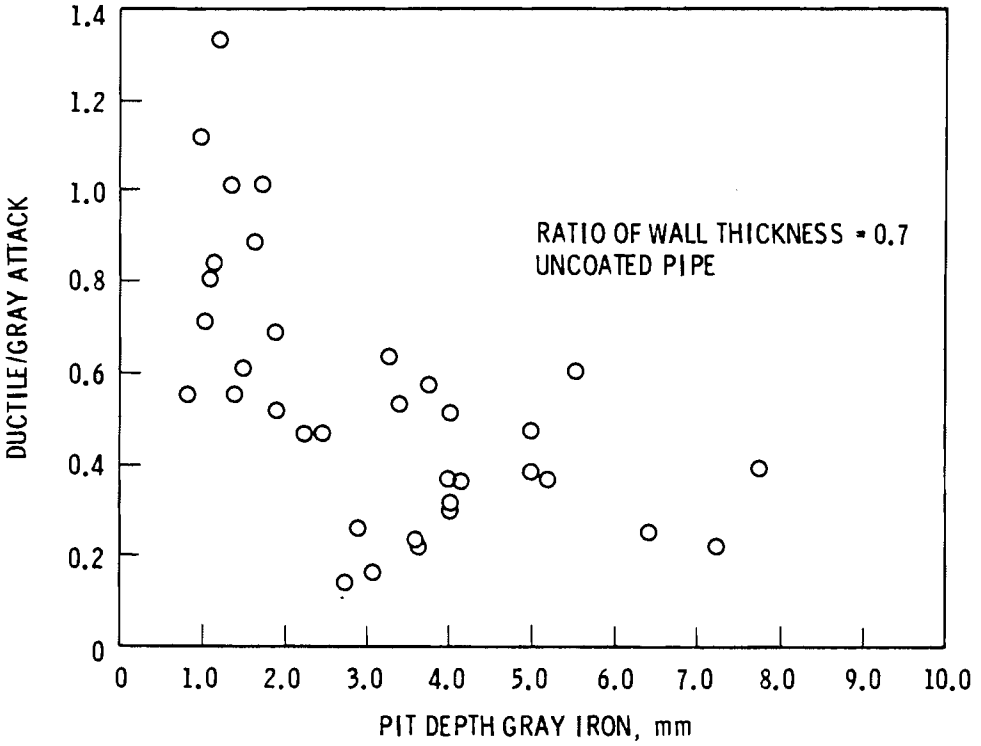

FIGURE 11. Relationship Between Maximum Pit Depth on Gray Iron Pipe Pipe and the Ratio of Attack, Ductile/Gray, for Pipes Buried in British, French, and German Sites (Reference 20)

Titanium Alloys

There are several reviews describing both pitting[56,57] and crevice corrosion[58,59] of titanium. The resistance of titanium in chloride solutions can be shown as a combination of chloride concentration and temperature, see Figure 12. According to this diagram, titanium should be resistant to pitting or crevice attack at ambient temperature in solutions of relatively high chloride content. As the temperature is increased, the probability for pitting and crevice attack increases. Beck[56] states that pitting of titanium occurs only in halide solutions and that corrosion can take place at ambient temperature depending on the anodic potential. The anodic potential at ambient temperature is about 8 V standard calomel electrode (SCE), which falls to about 1 V SCE at 473K. In bromide and iodide solutions, the potential is fairly constant with temperature at about 1 V SCE.

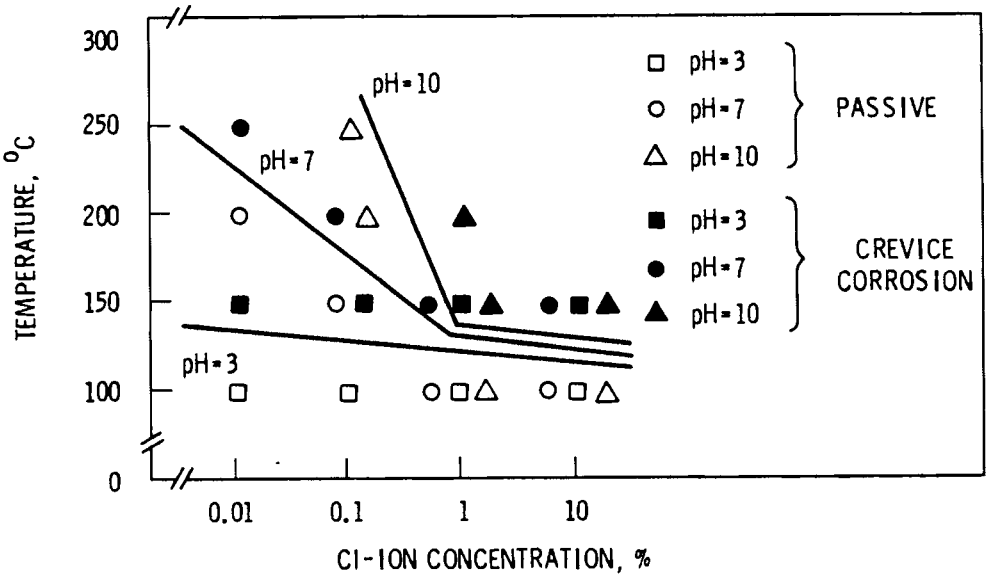

FIGURE 12. Crevice Corrosion and Passivity at Various pH Values, Cl^- Concentrations, and Temperatures (Reference 3)

The passive film breakdown potentials must be exceeded to initiate pitting attack; but, once an active corrosion reaction starts, the pitting potential will decrease to some critical value and further reduction in the potential can stop the pitting attack. Crevice corrosion can be initiated and continued at low anodic or cathodic potential.

Pitting or crevice attack is environment specific. The effect of environment on localized corrosion of titanium is summarized below.

- An increase in temperature will increase the probability for pitting and crevice attack, but the halide content of the solution will dictate the maximum use temperature of a specific titanium alloy. Crevice attack has not been seen at temperatures less than 373K (100°C).[58]
- Pitting corrosion on titanium occurs in halide environments; crevice corrosion is known to occur in both halide and sulfate environments.
- Decreasing the pH of the solution will tend to increase pitting and crevice attack; and increasing the pH above 8 will suppress attack, even at temperatures to 423K (250°C).[59] Figure 12 shows the effect of pH, chloride content, and temperature on crevice corrosion.

- Chloride concentrations up to 1 wt% may be tolerated by CP titanium at temperatures up to 513K.
- The effect of oxygen on pitting and crevice attack is not well defined. Takamura[60] compared the corrosion resistance of CP titanium and a Ti-0.2 Pd alloy in concentrated chloride solutions and found that the amount of oxygen in the creviced areas in CP titanium resulted in corrosion in that area. The corrosion resistance of the creviced Ti-Pd alloy was not lost in a low-oxygen chloride solution. The corrosion resistance in the Pd alloy case was not attributed to the passive TiO_2 film but to the accumulation of palladium at the surface, which developed a cathodic (protective) potential.[61] Charlot[44] exposed CP titanium to a deoxygenated, 473K, 3.4 wt% NaCl solution and saw no evidence of either pitting or crevice attack. Braithwaite et al.,[45] suggested from polarization data on CP Ti-grade 12 and Ti-0.2 Pd alloys in 513K sea water that the effect of oxygen on crevice corrosion reactions (i.e., anodic dissolution and the chloride reaction) would be small. Oxygen acts to repair defects in the passive oxide layer. No pitting or crevice attack was found on samples exposed in 522K sea water or brine under either oxidizing or deoxidizing conditions.
- Impurities on the titanium surface, iron in particular, have been found to enhance pitting attack.[62]

STRESS CORROSION CRACKING

Ferrous metals and titanium alloys can suffer failure by SCC when subjected to a combination of certain environments and mechanical tensile stress. One school of thought holds that SCC is due to the accelerated dissolution of metal at the crack tip. Cathodic polarization of the metal would help arrest the crack growth in this case. Hydrogen stress cracking is attributed to hydrogen atoms entering the metal at the crack tip, causing local embrittlement and subsequent crack growth. In this case, cathodic polarization worsens the situation and anodic polarization would help arrest crack growth. In many

metal failures it is difficult to separate hydrogen stress cracking from environmental stress cracking. Corrosion fatigue is a failure mode that combines the action of environment and stress. In corrosion fatigue the stress is cyclic rather than static; and when failures occur, they are generally at much lower stress levels than required in stress corrosion processes.

Cast Irons

Cast irons are generally not subject to SCC, and many of the failures of cast pipe in service have been attributed to either uniform or localized corrosion that reduced the structural integrity of the pipe to the point where failure occurred by mechanical overload.[21] In one case where a pipe was found to leak through a number of small cracks, it could not be determined whether the residual stress and corrosion caused the crack or if the cracks were already there causing the corrosion.[21]

Carbon steels do stress crack in a variety of environments depending on their yield strength and the tensile stresses imposed on them. The stress cracking of low-alloy steels has been reviewed elsewhere.[63,64] General observations made in these reviews for four specific aqueous environments are summarized below.

- aqueous chloride environments - Stress cracking of low-alloy steels in aqueous chloride environments is dependent on the yield strength of the alloy. At strengths less than about 689 MN/m^2 (100,000 psi) the steels are resistant to stress cracking; but as the strength of the material increases, so does the probability of stress cracking. Raising the chloride concentration in solution or increasing the temperature appears to have little effect on the SCC susceptibility as indicated by the environmental stress intensity factor;[a] however, an increase in either temperature or chloride concentration will accelerate crack growth. Highly acidic pH solutions accelerate

(a) The stress intensity factor is a value of the plane strain stress that will produce crack propagation by SCC of a given material in a given environment. It is derived from fracture mechanics principles.

SCC, but highly basic solutions restrict or stop crack initiation and propagation. Figure 13 shows the effect of pH on the stress intensity factor for a typical low-alloy steel. There is a substantial literature showing that SCC in chloride solutions is due to hydrogen embrittlement.

- nitrate solutions - Stress cracking of mild steels in nitrate solutions is dependent on the carbon content in the alloy. Generally the lower the carbon level, the greater the susceptibility. It has been shown that steels with pearlitic or spheroidized structure are more resistant to cracking. Very dilute nitrate solutions can cause cracking (640-ppm nitrate as NH_4NO_3) in mild steel at ambient temperature. An increase in either nitrate concentration or temperature decreases the resistance of the alloy to SCC.

- sodium hydroxide solutions - Stress cracking of steels in sodium hydroxide solutions (caustic cracking) is known to occur at temperatures from 373 to 623K. The lowest NaOH concentration causing SCC failures is about 5 wt%. Caustic cracking is generally accelerated by small amounts of oxygen; but, as the oxygen content increases, the susceptibility of the metal to cracking decreases. Silicates, sulfates, and carbonates tend to inhibit caustic cracking of low-alloy steels.

- carbonate solutions - Stress cracking of medium-strength low-alloy steels (689 to 1034 MN/m^2) in carbonate solutions occurs within a limited range of electrochemical potential. A mild steel showed failure in an ammonium carbonate solution of pH between 8 and 10 at potentials between -450 and -625 mV SCE. As the temperature was increased, the potential susceptibility band narrowed.[65] Generally, low-alloy steels will be resistant in carbonate solutions; but when concentration, temperature, and potential conditions are right, carbon steels can SCC.

Titanium Alloys

The SCC resistance of CP or low-alloy alpha titanium in aqueous solutions is generally considered excellent. Stress cracking of titanium has been a

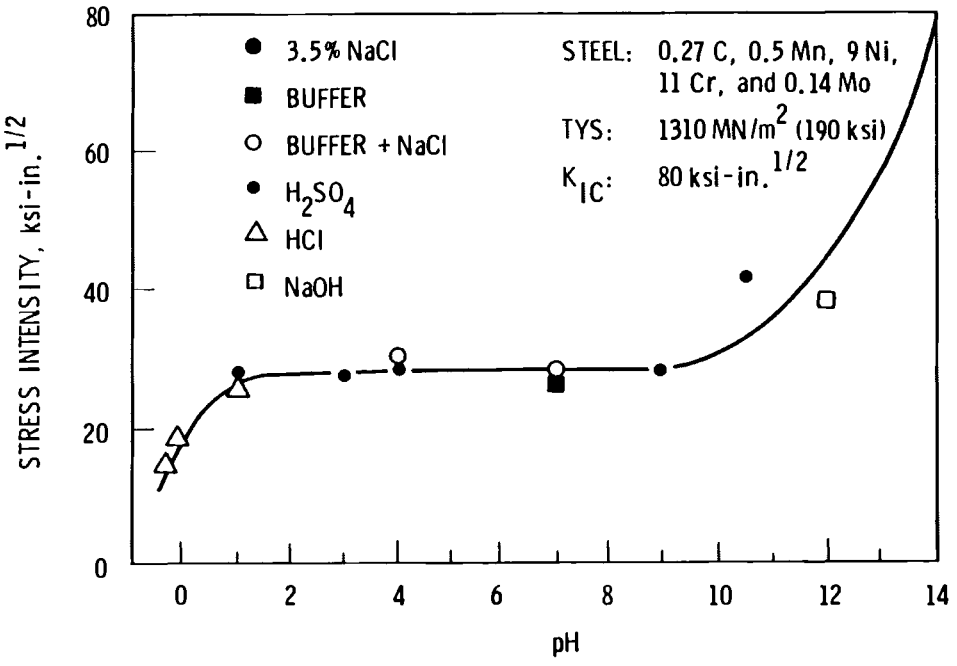

ENVIRONMENT	pH
2 N HCl	0.3
N HCl	0
N/10 HCl	1
N/10 H_2SO_4	1
BDH BUFFER	3.1
BDH BUFFER	4.0
BDH BUFFER + 3.5% NaCl	4.0
BDH BUFFER	7.0
BDH BUFFER + 3.5% NaCl	7.0
3.5% NaCl	7.0
BDH BUFFER	9.2
BDH BUFFER	11.4
N/10 NaOH	13.0
1 N NaOH	14.0

FIGURE 13. Effect of pH on the Threshold Stress Intensity (Reference 65)

problem when the strengths of the alloy had to be improved by element addition or heat treatments. Table 14 shows the relative susceptibility of several titanium alloys in a saltwater environment.

Solutions containing halides have shown a tendency to accelerate SCC in susceptible alloys or to induce SCC susceptibility in alloys normally immune in distilled water. There are a number of reviews discussing the stress corrosion of titanium.[66-70] The comments listed below are specific to the CP titanium or low-alloy alpha materials in an aqueous environment.

- Oxygen, iron, and aluminum have been singled out for their adverse effect on the SCC resistance of titanium. Oxygen and iron are difficult to remove from unalloyed titanium and exist as major impurities in the metal. Aluminum is the most prominent alloying element in titanium, and the Ti-6 Al-4 V alloy is probably the most widely used. As oxygen is increased in the CP grades of titanium, the resistance to SCC decreases.[71] CP Ti-50 A is essentially immune to SCC whereas Ti-75 A and Ti-100 A are considered moderately susceptible.[72] Table 15 shows the loss of SCC resistance in unalloyed titanium as the oxygen content exceeds about 0.2 wt%.
- The relative SCC susceptibility of the alpha alloys is determined by a combination of their strength and stable microstructure. The iron impurity in most titanium alloys can cause an "omega" phase to form that promotes SCC susceptibility.[67] This phase is dependent on the thermal history of the alloy and/or any residual beta (BCC phase) in the alpha (HCP) structure.
- Aqueous SCC of titanium generally occurs in susceptible alloys having a pre-existing crack-like flaw. Prenotch or precrack specimens are normally used to evaluate the susceptibility of an alloy. The passive TiO_2 film insulates and protects the metal from the environment, preventing crack initiation and growth. However, when either the environment (hot brine or low pH, halide solutions) or stress level prevents passivation, SCC failure can occur. The mechanisms for crack propagation include the role of both hydrogen and chloride ions.

TABLE 14. Stress Corrosion Susceptibility of Titanium Alloys in 3.5% NaCl Solutions[a]

Test solution:	3.5% NaCl solution pH 8 or synthetic sea salt[b]
Test temperature:	ambient
Specimen type:	cantilever beam, notched, and with and without crack initiated at base of notch by fatigue
Failure time:	less than 1 h at critical load
Type of cracking:	intergranular and transgranular
Alloys that are sensitive:	unalloyed RS-70 (annealed)[c] Ti-7 Al-2 Cb-1 Ta (annealed) Ti-7 Al-3 Cb (annealed) Ti-6 Al-2.5 Sn (annealed) Ti-5 Al-2.5 Sn (annealed Ti-6 Al-3 Cb-2 Sn (annealed) Ti-7 Al-3 Cb-2 Sn (annealed) Ti-8 Al-3 Cb-3 Sn (annealed) Ti-8 Mn (annealed) Ti-8 Al-1 Mo-1 V (slightly) (annealed) Ti-6 Al-4 V (very slightly) (annealed) Ti-6.5 Al-5 Zr-1 V (aged at 1100°F) Ti-6 Al-4 V-1 Sn (aged at 1100°F) Ti-6 Al-6 V-2.5 Sn (aged at 900°F) Ti-6 Al-2 Mo (aged at 1100°F) Ti-7 Al-3 Mo (annealed) Ti-13 V-11 Cr-3 Al (annealed)
Alloys that are not sensitive:	Ti-65 A (annealed) Ti-6 Al-4 V (annealed and annealed and aged) Ti-7 Al-2.5 Mo (annealed) Ti-6 Al-2 Mo (annealed) Ti-6 Al-2 Sn-1 Mo-1 V (annealed) Ti-6.5 Al-5 Zr-1 V (annealed) Ti-6 Al-2 Sn-1 Mo-3 V (annealed) Ti-5 Al-2 Sn-2 Mo-2 V (annealed) Ti-6 Al-2 Cb-1 Ta-0.8 Mo (annealed) Ti-4 Al-3 Mo-1 V (age hardened) Ti-13 V-11 Cr-3 Al (age hardened)

(a) Reference 69.
(b) ASTM Specifications for Substitute Ocean Water (D 1141-52).
(c) RS-70 alloy is comparable to commercial Ti-Grade 2.

TABLE 15. Effect of Oxygen on the Aqueous Stress Corrosion of Titanium[a]

Composition	Failure Stress-Intensity K, ksi $\sqrt{in.}$		Ratio of Seawater Test to Air Test
	In Air	In Sea Water	
Ti-0.060% O[b]	52.9	51.4	0.97
Ti-0.20% O[b]	72.3	68.0	0.94
Ti-0.40% O[b]	90.3	53.3[c]	0.59
Ti-0.40% O + 1.0% Mo[b]	99.4	62.5[c]	0.63
Ti-6% Al-4% V-0.08% O[c]	93	88	0.95
Ti-6% Al-4% V-0.18% O[c]	92	60[d]	0.65

(a) Reference 72.
(b) Annealed: 1300°F, 7 h, vacuum cooled.
(c) Fracture texture showed stress corrosion.
(d) Annealed: 1450°F, 8 h, furnace cooled.

Hydrogen is known to play an active role in SCC. Apart from that role, hydrogen readily reacts with titanium to form a stable hydride phase that in turn affects the impact properties of the alloy. Figure 14 shows this effect for unalloyed titanium and the Ti-6 Al-4 V alloy. Hydrogen embrittlement becomes more severe with increased hydrogen content, increased strain rate, decreased temperature (over a narrow range), and in notched or precracked metal parts. While the titanium matrix can accept and tolerate certain levels of hydrogen without embrittlement, temperature and stress gradients in the metal can redistribute the hydride phase leading to delayed fracture.

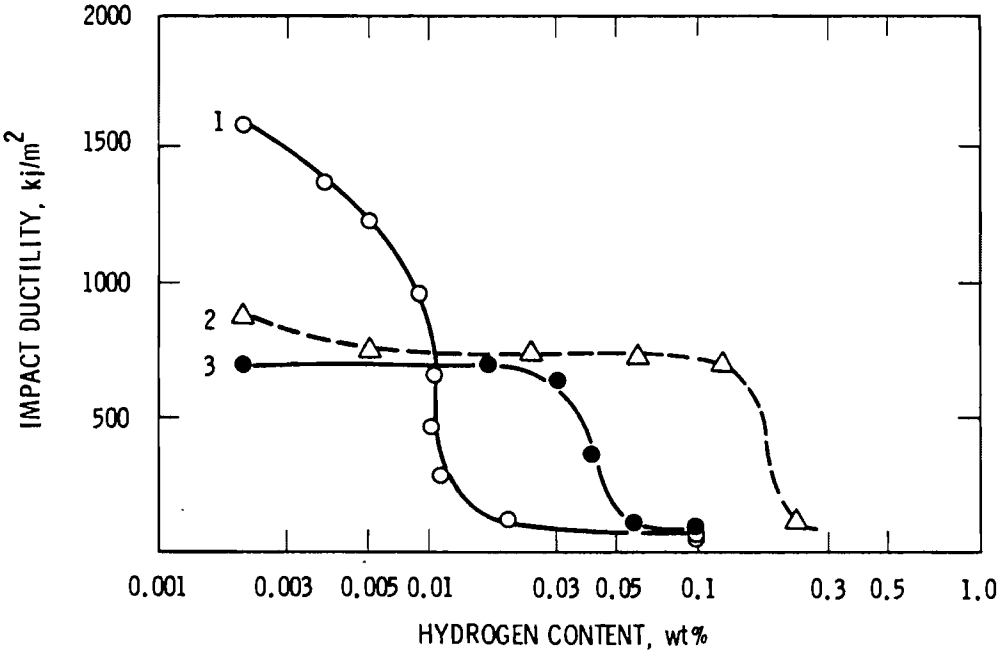

FIGURE 14. Effect of Hydrogen on Impact Ductility of Titanium Alloys. Line 1: Ti; line 2: Ti-6 Al-4V; line 3: 5 Al-2 Sn (Reference 73).

CORROSION RESISTANCE OF REFERENCE METALS IN A BASALT ENVIRONMENT

THE BASALT ENVIRONMENT

Any waste package that is stored and sealed in an underground repository will be subject to the local chemistry of the geology changed somewhat by the heat and radiation generated by the waste form contained within the package. In a basalt repository, one would expect a continual but slow movement of ground water as an aqueous phase through the site. The chemistry of the ground water is important when either experimentally assessing the suitability of candidate barrier metals or trying to relate literature data to the probable barrier metal-environment interactions. An analysis of the Grande Ronde basalt flow ground water is shown in Table 16.

Oxygen content and solution pH are two important parameters when considering the passive nature of oxide films on metals, particularly for cast irons. The analysis in Table 16 shows no oxygen content; it is generally accepted that in a sealed deep basalt repository the oxygen content will be reduced to very low levels (to an oxygen activity approximately comparable to the Ni/NiO equilibrium). The bulk solution pH in the Grande Ronde waters is about 9.9 at 298K, but the repository pH will be dictated by the carbonate-bicarbonate-silica reactions at the temperatures developed near the waste package (that is, a pH of 7.5 at 473K). The choice of backfill may also affect the solution chemistry near the waste package.

If the high-temperature potential-pH diagrams (Figure 7 for iron-water and Figure 4 for titanium-water) are compared, it can be seen that the pH of the Grande Ronde water chemistry puts these metals in the passive corrosion area. If the passive layer remains protective, metal loss will be by slow uniform corrosion. The reasonably low levels of chloride, fluoride, and sulfate ions in the ground water suggest that the Grande Ronde will be a fairly nonaggressive environment from a metals corrosion view although there may be some concern about whether the fluoride ion will contribute to nonuniform corrosion.

TABLE 16. Comparison of Actual and Synthetic Grande Ronde Ground-Water Compositions at 298K[a]

Chemical Species	Actual Composition, mg/l	Actual Composition, epm[c]	Synthetic Composition,[b] mg/l	Synthetic Composition,[b] epm
Na^{+}	250	10.875	263	11.430
K^{+}	1.9	0.049	1.9	0.049
Ca^{+2}	1.3	0.065	1.3	0.065
Mg^{+2}	0.04	0.033	0.04	0.033
Total Cation Equivalence		11.022		11.577
CO_3^{-2}	27	0.897	27	0.897[d]
HCO_3^{-}	70	1.152	70	1.152[d]
OH^{-}	1.4	0.083	1.4	0.083[d]
$H_3SiO_4^{-}$[e]	103	1.080	103	1.080[d]
Cl^{-}	148	4.174	148	4.167
SO_4^{-2}	108	2.249	109	2.260
F^{-}	37	1.947	37	1.950
Total Anion Equivalence		11.582		11.589

(a) Reference 5.
(b) This composition conforms to a solution pH of ≈9.92.
(c) epm = equivalents per million.
(d) Based on an epm of 3.212.
(e) Based on a total dissolved SiO_2 content of 121 mg/l.

ASSESSMENT OF CAST IRONS IN A BASALT ENVIRONMENT

When low-alloy cast irons are used as a metal barrier, they must be used in relatively thick sections to account for the corrosion allowance that must be applied. Availability, cost, and fabricability are among those features of cast irons that might make their use potentially acceptable in a basalt repository. The corrosion data found in the literature were not entirely suitable for recommending one grade or type of cast iron over another. Comparisons were generally made betweeen gray cast irons (flake graphites) and ductile irons (nodular graphites). It would seem reasonable that the metal barrier should have the degree of strength, ductility, and impact resistance afforded by the nodular irons.

It became apparent that elevated temperature aqueous corrosion data do not exist in the literature for cast irons; corrosion data for carbon steels at high temperature were taken from the literature and reported in this document. The carbon or low-alloy steel data can, however, be applied to the high-temperature corrosion of cast irons with some confidence because of the general agreement in corrosion mechanisms and in some cases corrosion rates in the temperature regime of 323 to 573K.

The uniform corrosion rate that might be expected in 523K basalt ground water will probably fall within the parabolic rates extrapolated from McEnaney's[29] data on gray cast iron, the linear rate after the passive film has formed on mild steels in alkaline hydroxides,[36] and the linear rate of carbon steels in neutral pH, high-purity, deoxygenated flow water.[34] Table 17 compares an estimated metal penetration after 500 and 1000 yr from these data and shows the average uniform corrosion rates of cast iron in a medium-resistivity soil.

If the usual corrosion allowance of a factor of five were applied, the cast iron barrier should be between 0.18 and 0.33 mm (7 and 13 in.) thick to last 1000 yr. Corrosion allowances are normally applied to account for the loss in strength as the metal is affected by the environment. A factor of five allowance may be too high in the engineered barrier design; if so, a lesser wall thickness could be used.

TABLE 17. Estimated Uniform Metal Penetration in Cast Iron and Carbon Steel

Reference	Rate Law	Temperature, K	Environment	Penetration, mm 500 yr	1000 yr
29	Parabolic[a]	523	pH 7 to 8 H_2O	28	38
36	Linear[b]	523	13% NaOH	20	38
34	Linear[b]	523	Neutral H_2O	33	66
22	Linear[c]	Ambient	Soil	25	51

(a) The weight change used in determining this rate expression comprises both the iron lost to the environment and iron left on the metal as corrosion product.
(b) The corrosion rate based on weight gain (corrosion product growth) after the initial rapid corrosion. The data do not consider metal lost to the system due to the solubility of the corrosion film.
(c) Descaled weight loss data after 10 yr underground.

Failure of cast iron pipes in a soil (underground) medium is generally dictated by localized rather than uniform corrosion; and the more aggressive soils are those containing high oxygen, chloride, and sulfate concentrations. In the basalt environment the oxygen will be low, but both chloride and sulfate concentrations are about at the level where passive film breakdown might occur. McEnaney[31] did not see pitting in tests with solutions containing about the same level of chloride and sulfate as the basalt ground water, and localized corrosion was not reported in the high-temperature data on the corrosion of low-alloy carbon steel.[37] If pitting should occur on the cast iron barrier, it would be expected to be no worse than the average pit depths reported for cast iron in soils. For example, gray irons, which have poorer resistance to localized corrosion than nodular irons, that were exposed in a clay soil for 11 yr showed maximum pit depths of 3.0 mm (117 mil). It is tempting to assume a pit growth rate of 1 mpy and to extrapolate this to 1000 yr showing, in this case, that pitting is no worse than uniform corrosion. It should be remembered, however, that pitting can be accelerated or stopped by the local chemistry around the metal and that such extrapolations will be guesses at best. We would expect that localized corrosion in the basalt ground waters will not be worse than uniform corrosion.

Low-alloy cast irons should not be susceptible to SCC or hydrogen stress cracking. The normal strength of these materials is below the strength levels in ferrous metals known to fail by a SCC mechanism. If cracking should occur in cast irons, it will probably be the result of mechanical overload failure resulting from a uniform corrosion that reduces the cross section of the load-supporting metal or from a lack of impact resistance.

ASSESSMENT OF TITANIUM ALLOYS IN A BASALT ENVIRONMENT

Provided that the strength requirements for the engineered barrier allows the use of low-alloy titanium metals, they would be acceptable as candidate alloys based on their corrosion resistance. The literature assessment by Pettersson[3] and the experimental work of Braithwaite[45] show that commercial titanium, Ti-grade 12, or Ti-2 Pd alloys could be effective long-lived barriers.

In a basalt environment the corrosion of titanium should be in the passive region. Uniform corrosion is expected to be very low, averaging less than 0.004 mpy based on high-temperature alkaline water data. If deoxygenated sea water or 3 wt% NaCl solution data are used, uniform corrosion rates will probably average less than 0.1 mpy. We would expect the corrosion rates to be closer to the 0.004-mpy rate. If these two rates are arbitrarily averaged and linear growth over 1000 yr at temperature is assumed, only about 50 mils of the metal would be corroded. If a corrosion factor of five is applied, a 0.25-in. thick titanium barrier would be required to protect the waste form.

Localized corrosion in the form of pitting and crevice attack is not considered to be an active form of corrosion to Ti alloys in the basalt environment. At the high pH level of the basalt ground water, the concentration of chloride (the most active species causing pitting and crevice attack) needed to initiate pitting attack (affect passivation) is greater than 1 wt% for CP titanium alloy at $T > 200^{o}C$; Braithwaite[45] has shown the considerable pitting resistance of the Ti-2 Pd or Ti-grade 12 alloys in high-temperature brine solutions.

The low-oxygen CP titanium alloys offer excellent SCC resistance in aqueous environments. A stress cracking failure mode for the low-alloy titanium metals is not expected in the basalt environment. Hydrogen stress cracking, where the environment supplies hydrogen to the metal, is also not anticipated as long as the metal remains in the passive state. The embrittlement of titanium alloys by internal hydrogen (i.e., the redistribution of hydrogen in some stress state causing delayed failure) is a potential problem, but it is beyond the scope of this review. Delayed failure is known to occur in titanium, particularly in the alpha-beta alloys.

REFERENCES

1. Report to the President by the Interagency Review Group on Nuclear Waste Management. TID-29442, March 1979.

2. Allard, B., et al. 1979. "Disposal of Radioactive Waste in Granitic Bedrock." In Radioactive Waste in Geologic Storage, ACS Symposium Series 100, p. 47.

3. Henriksson, S., and K. Pettersson. 1977. An Investigation Concerning the Suitability of Titanium as a Corrosion Resistant Canister for Nuclear Waste. KBS Technical Report 11, Aktie bolaget Atomenergi, Sweden, ORNL-tr-4648.

4. Oriani, R. A., and P. H. Josephic. 1979. "Hydrogen-Assisted Crack Initiation in a High-Strength Steel." In Environment-Sensitive Fracture of Engineering Materials, ed. Z. A. Foroulis, p. 440. The Metallurgical Society of AIME.

5. Wood, M. I. 1980. BWIP Data Package for Reference Data of Groundwater Chemistry. RSD-BWI-007, Rockwell Hanford Operations, Richland, Washington.

6. Angus, H. T. 1978. Cast Iron: Physical and Engineering Properties. Butterworths, Boston, Massachusetts.

7. Merchant, H. D., ed. 1968. Recent Research on Cast Iron. Gordon and Breach, New York.

8. American Society for Metals. 1979. Metals Handbook. Vol. 1, Selection and Properties, 8th ed., pp. 349-406, 524-537.

9. Wallace, J. F. 1968. Engineering Properties of Cast Iron. SP66-68, American Society of Tool and Manufacturing Engineers, Dearborn, Michigan.

10. Heine, H. J. 1969. Gray, Ductile, and Malleable Iron Casting--Current Capabilities. ASTM STP 455, Philadelphia, Pennsylvania.

11. Battelle Columbus Laboratories. 1980. Mechanical Properties Data Center, Structural Alloys Handbook, Vol. 1. Columbus, Ohio.

12. Pearce, J. G. 1942. Trans. Inst. Welding 5:156.

13. Jaffee, R. I., and N. E. Promisel, eds. 1970. The Science, Technology and Application of Titanium. Pergamon Press, New York.

14. Engineering Alloys Digest, Inc. 1978. Alloy Digest. Montclair, New Jersey.

15. Hall, J. A. 1977. A Review of Titanium Alloys for Engineering Applications and Corrosion Resistance. TIMET, Henderson, Nevada.

16. National Association of Corrosion Engineers. 1980. NACE Corrosion Engineers Reference Book. Houston, Texas, p. 155.

17. Pourbaix, M. 1973. Lectures on Electrochemical Corrosion. Plenum Press, New York.

18. Pourbaix, M. 1966. Atlas of Electrochemical Equilibrium in Aqueous Solutions. Pergamon Press, New York.

19. Garrels, R. M., and C. L. Christ. 1965. Solutions, Minerals, and Equilibria. Freeman, Cooper and Co., San Francisco, California.

20. Fuller, A. G. 1976. "Comments on 'Corrosion Behavior of Ductile Cast-Iron Pipe in Soil Environments'." J. Am. Water Works Assoc., December 1976, p. 111.

21. Office of Pipeline Safety. 1971. Ferrous Pipeline Corrosion Processes, Detection, and Mitigation. Tech. Report OPS-TR-71-001, Washington, D.C.

22. Logan, K. H. 1945. Underground Corrosion. National Bureau of Standards Circular C450, Washington, D.C.

23. Romanoff, M. 1964. "Exterior Corrosion of Cast Iron Pipe," J. Am. Water Works Assoc. September 1964, p. 1129.

24. Romanoff, M. 1968. "Performance of Ductile Iron Pipe in Soils." J. Am. Water Works Assoc. June 1968, p. 645.

25. Crews, D. L. 1976. "Comments on 'Corrosion Behavior of Ductile Cast-Iron Pipe in Soil Environments'." J. Am. Water Works Assoc. December 1976, p. 112.

26. Bureau of Reclamation. March 1965. Corrosion of Some Ferrous Metals in Soil with Emphasis on Mild Steel and Grey and Ductile Cast Irons. U.S. Department of Interior, Washington, D.C.

27. Hudson, J. C., and K. O. Watkins. 1968. Tests on the Corrosion of Buried Cast Iron and Mild Steel Pipes. British Iron and Steel Research Association, London.

28. Uhlig, H. H. Corrosion Handbook. John Wiley and Sons, Inc., New York.

29. McEnaney, B., and D. C. Smith. 1978. "Corrosion of a Cast Iron Boiler in a Model Central Heating System." Corrosion Science 18:519.

30. Potter, E. C., and G.M.W. Mann. 1961. 1st International Congress on Metallic Corrosion. Butterworths, London, p. 417.

31. Smith, D. C., and B. McEnaney. 1979. "The Influence of Dissolved Oxygen Concentration on the Corrosion of Grey Cast Iron in Water at 50°C." Corrosion Science 19:379.

32. Schaschl, E., and G. A. Marsh. 1974. "The Placement of Reference Electrode and Impressed Current Anode Effect on Cathodic Protection of Steel." Materials Performance 13:13-16.

33. Townsend, H. E., Jr. 1969. "Potential-pH Diagrams at Elevated Temperature for the System Fe-H_2O." In Proceedings of 4th International Congress on Metallic Corrosion, p. 477.

34. Pocock, F. J. 1979. "Corrosion and Contaminant Control Concerns in Central Station Steam Supply Systems." J. Materials for Energy Systems 1:3.

35. Pearl, W. L., and G. P. Wozadlo. 1965. "Corrosion of Carbon Steel in Simulated Boiling Water and Superheat Reactor Environments." Corrosion 21:260.

36. Asai, O., and N. Kawashima. 1969. "Corrosion of Mild Steel in High Temperature and Pressure Water." In Proceedings of 4th International Congress on Metallic Corrosion, p. 492.

37. Mann, G.M.W. 1976. "The Oxidation of Iron Base Alloys Containing Less than 12Δ Cr in High Temperature Aqueous Solutions." High Temperature High Pressure Electrochemistry in Aqueous Solutions, NACE-4, National Association of Corrosion Engineers, Houston, Texas.

38. Berry, W. E. 1971. Corrosion in Nuclear Applications. John Wiley, New York.

39. Hurlen, T. 1960. "Oxidation of Titanium." J. Inst. Met. 89:129.

40. Cox, B., and K. Alcock. 1959. The Oxidation of Zirconium and Its Alloys. VII. Experience with High Pressure Equipment for Use with Aqueous Solutions at High Temperatures. UKAEA Report, AERE-R3029, Harwell, England.

41. Trach, J. D., and R. H. Meservey. 1972. Corrosion of Thermocouple Sheath Materials in a Pressurized Water Reactor Environment. ANCR 1033, Aerojet Nuclear Company, Idaho Falls, Idaho.

42. Straumanis, M. E., and P. C. Chen. 1959. "The Corrosion of Titanium in Acids." Corrosion 7:229.

43. Sanderson, B. T., and M. Romanoff. 1969. "The Performance of Commercially Pure Titanium in Soils." In Proc. of the 25th NACE Conference, Houston, Texas, p. 2.

44. Charlot, L. 1970. Investigation of Galvanically Induced Hydriding of Titanium in Saline Solutions. R&D Report 624, U.S. Dept. of Interior, Washington, D.C.

45. Braithwaite, J. W., N. J. Magnani, and J. W. Muniford. 1980. Titanium Alloy Corrosion in Nuclear Waste Environments. SAND 79 2023C, Sandia Laboratories, Albuquerque, New Mexico.

46. Feniberg, I. J., and M. L. Pickelsimer. 1972. Examination of Failed Six Inch Cast Iron Pipe Gas Main. NBS 312.01/56, National Bureau of Standards, Washington, D.C.

47. Pickelsimer, M. L. 1972. Examination of Failed Four Inch Cast Iron Pipe Gas Main. NBS 312.01/49, National Bureau of Standards, Washington, D.C.

48. Shives, T. R. 1972. Examination of Failed Ten Inch Cast Iron Pipe Gas Main. NBS 312.01/55, National Bureau of Standards, Washington, D.C.

49. McBee, C. L., and J. Kruger. "Events Leading to the Initiation of the Pitting of Iron." Localized Corrosion, NACE-3, National Association of Corrosion Engineers, Houston, Texas, p. 252.

50. Ashworth, V., et al. 1970. "On the Cl Breakdown of Passive Films on Mild Steel." Corrosion Science 10:481.

51. Wranglen, G. 1969. "Review Article on the Influence of Sulfide Inclusions on the Corradability of Iron and Steel." Corrosion Science 9:588.

52. Wranglen, G. 1974. "Active Sulfides and the Pitting Corrosion of Carbon Steels." In Localized Corrosion, NACE-3, National Association of Corrosion Engineers, Houston, Texas, p. 462.

53. Wallwork, G. R., and B. Harris. 1974. "Localized Corrosion in Mild Steel." Localized Corrosion, NACE-3, National Association of Corrosion Engineers, Houston, Texas, p. 292.

54. Pickering, H. W., and R. P. Frankenthal. 1974. "Mechanism of Pit and Crevice Propagation on Iron and Stainless Steels." Localized Corrosion, NACE-3, National Association of Corrosion Engineers, Houston, Texas, p. 261.

55. Shreir, L. L., ed. 1976. Corrosion. Vol. 1, Newnes-Butterworths, London, p. 3:92.

56. Beck, T. R. 1974. "A Review: Pitting Attack of Titanium Alloys." Localized Corrosion, NACE-3, National Association of Corrosion Engineers, Houston, Texas, p. 644.

57. Cotton, J. B. 1974. "A Perspective View of Localized Corrosion of Titanium." Localized Corrosion, NACE-3, National Association of Corrosion Engineers, Houston, Texas, p. 676.

58. Gleekman, L. W. 1974. "Historical Industrial Developments with Crevice Corrosion of Titanium." Localized Corrosion, NACE-3, National Association of Corrosion Engineers, Houston, Texas, p. 669.

59. Jackson, J. D., and W. K. Boyd. 1968. "Crevice Corrosion of Titanium." Applications Related Phenomena in Titanium Alloys, ASTM STP 432, Philadelphia, Pennsylvania, p. 218.

60. Takamura, A. 1967. "Corrosion Resistance of Ti and a Ti-Pd Alloy in Hot, Concentrated Sodium Chloride Solutions." Corrosion October 1967, p. 306.

61. Cotton, J. B. 1967. "The Role of Palladium in Enhancing the Corrosive Resistance of Titanium." Platinum Metals Review 11:50.

62. Syrett, B. C., D. D. MacDonald, and H. Shih. "Pitting Resistance of Engineering Materials in Geothermal Brines--1. Low Salinity Brine." Corrosion 36:130.

63. Okada, H. "Stress Corrosion Cracking and Hydrogen Cracking of Structural Steels." Stress Corrosion Cracking and Hydrogen Embrittlement of Iron Base Alloys, NACE-5, National Association of Corrosion Engineers, Houston, Texas, p. 124.

64. Carter, C. S., and M. V. Hyatt. "Review of Stress Corrosion Cracking in Low Alloy Steels with Yield Strengths Below 150 ksi." Stress Corrosion Cracking and Hydrogen Embrittlement of Iron Base Alloys, NACE-5, National Association of Corrosion Engineers, Houston, Texas, p. 524.

65. Parkins, R. N. "Environmental Aspects of Stress Corrosion Cracking in Low Strength Ferritic Steels." Stress Corrosion Cracking and Hydrogen Embrittlement of Iron Base Alloys, NACE-5, National Association of Corrosion Engineers, Houston, Texas, p. 601.

66. Feige, N. G., and L. C. Covington. 1972. "Overview of Corrosion Cracking of Titanium Alloys." Stress Corrosion Cracking of Metals: A State of the Art, ASTM STP 518, p. 119.

67. Brown, B. F. 1977. Stress Corrosion Cracking Control Measures. National Bureau of Standards, Monograph 156, Washington, D.C.

68. Jaffee, R. I., and N. E. Promisel. 1973. The Science, Technology and Application of Titanium. Pergamon Press, New York, pp. 239-324.

69. Blackburn, M. J., J. A. Feeney, and T. R. Beck. 1973. "Stress Corrosion Cracking of Titanium Alloys." Advances in Corrosion Science and Technology, Vol. 3, Plenum Press, New York, p. 67.

70. Scully, J. C., and D. T. Powell. 1970. "The Stress Corrosion Cracking Mechanism in Alpha Titanium Alloys at Room Temperature." Corrosion Science 10:719.

71. Scully, J. C., and T. A. Adepoju. 1977. "Stress Corrosion Crack Propagation in a Ti-O Alloy in Aqueous and Methanolic Solutions." Corrosion Science 17:789.

72. Seagle, S. R., R. R. Seeley, and G. S. Hall. 1968. "The Influence of Composition and Heat Treatment on the Aqueous Stress Corrosion of Titanium." Applications Related Phenomena in Titanium Alloys, ASTM STP 432, Philadelphia, Pennsylvania, p. 170.

73. Beevers, C. J., M. R. Warren, and D. V. Edmonds. 1973. "The Temperature Dependence of Fracture Behavior in Alpha-Titanium-Hydrogen Alloys." The Science and Technology and Application of Titanium, Pergamon Press, New York, p. 557.

74. Strehblow, H. H., B. Titze, and B. P. Loechel. 1979. "The Breakdown of Iron and Nickel by Fluoride." Corrosion Science 19:1047.

DISTRIBUTION

No. of Copies

OFFSITE

A. A. Churm
DOE Chicago Patent Division
9800 South Cass Avenue
Argonne, IL 60439

T. C. Chee
Office of Waste Operations and Technology
DOE Nuclear Waste Management
Washington, DC 20545

2 G. H. Daly
Office of Waste Operations and Technology
DOE Nuclear Waste Management (NE-322)
Germantown, MD 20545

J. E. Dieckhoner
Office of Waste Operations and Technology
DOE Nuclear Waste Management (NE-321)
Germantown, MD 20545

D. J. McGoff
Office of Waste Operations and Technology
DOE Nuclear Waste Management (NE-323)
Germantown, MD 20545

G. Oertel, Director
Office of Waste Operations and Technology
DOE Nuclear Waste Management (NE-320)
Germantown, MD 20545

C. R. Cooley
Office of Waste Isolation
DOE Nuclear Waste Management (NE-331)
Washington, DC 20545

No. of Copies

C. A. Heath
Office of Waste Isolation
DOE Nuclear Waste Management (NE-330)
Germantown, MD 20545

S. Meyers/R. Romatowski
DOE Nuclear Waste Management (NE-30)
Germantown, MD 20545

A. F. Perge
DOE Nuclear Waste Management (NE-30)
Washington, DC 20545

R. D. Walton
MSB-107
DOE Division of Waste Products
Germantown, MD 20545

W. E. Mott
DOE Division of Environmental Control Technology
Washington, DC 20545

R. E. Cunningham
Deputy Director for Fuels and Materials
U.S. Nuclear Regulatory Commission
Silver Springs, MD 20910

D. M. Rohrer
U.S. Nuclear Regulatory Commission
Washington, DC 20555

2 S. W. Ahrends
DOE Oak Ridge Operations Office
Oak Ridge, TN 37830

2 E. S. Goldberg
DOE Savannah River Operations Office
P.O. Box A
Aiken, SC 29801

No. of Copies

J. P. Hamric
DOE Idaho Operations Office
550 2nd Street
Idaho Falls, ID 83401

2 S. G. Harbinson
DOE San Francisco Operations
1333 Broadway
Oakland, CA 94612

T. B. Hindman, Jr.
DOE Savannah River Operations Office
P.O. Box A
Aiken, SC 29801

DOE Los Alamos Scientific Laboratory
P.O. Box 1663
Los Alamos, NM 87544

2 R. Y. Lowrey
DOE Albuquerque Operations Office
Albuquerque, NM 87115

S. A. Mann
DOE Chicago Operations and Regional Office
Argonne, IL 60439

J. Neff, Program Manager
DOE Columbus Program Office
505 King Avenue
Columbus, OH 43201

John Van Cleve
DOE Oak Ridge Operations Office
P.O. Box X
Oak Ridge, TN 37830

2 J. B. Whitsett
DOE Idaho Operations Office
550 2nd Street
Idaho Falls, ID 83401

No. of Copies

27 DOE Technical Information Center

A. Williams
Allied-General Nuclear Service
P.O. Box 847
Barnwell, SC 29812

J. L. Jardine
Argonne National Laboratory
9700 South Cass Avenue
Argonne, IL 60439

J. H. Kittel
Office of Waste Management Programs
Argonne National Laboratory
9700 South Cass Avenue
Argonne, IL 60439

M. J. Steindler
Chemical Engineering Div.
Argonne National Laboratory
9700 South Cass Avenue
Argonne, IL 60439

M. M. Steindler/L. E. Trevorrow
Argonne National Laboratory
9700 South Cass Avenue
Argonne, IL 60439

Wayne Carbiener
Office of Nuclear Waste Isolation
Battelle-Columbus Laboratories
505 King Avenue
Columbus, OH 43201

2 J. Carr
Office of Nuclear Waste Isolation
Battelle Memorial Institute
505 King Avenue
Columbus, OH 43201

No. of Copies

2 J. F. Kircher
Office of Nuclear Waste Isolation
Battelle Memorial Institute
505 King Avenue
Columbus, OH 43201

2 D. T. Moak
Office of Nuclear Waste Isolation
Battelle Memorial Institute
505 King Avenue
Columbus, OH 43201

Beverly Rawles
Office of Nuclear Waste Isolation
Battelle Memorial Institute
505 King Avenue
Columbus, OH 43201

J. W. Voss
Office of Nuclear Waste Isolation
Battelle Memorial Institute
505 King Avenue
Columbus, OH 43201

Brookhaven National Laboratory
Reference Section
Information Division
Upton, NY 11973

H. Henning
Electric Power Research Institute
P.O. Box 10412
Palo Alto, CA 94301

Environmental Protection Agency
Technology Assessment Division (AW-559)
Office of Radiation Programs
Washington, DC 20460

No. of Copies

J. R. Berreth
Exxon Nuclear Idaho Corp.
P.O. Box 2800
Idaho Falls, ID 83401

Exxon Nuclear Corporation
(File Copy)
P.O. Box 2800
Idaho Falls, ID 83401

Larry L. Hench
Dept. of Materials Science and Engineering
University of Florida
Gainesville, FL 32611

R. G. Barnes
General Electric Company
175 Curtner Avenue (M/C 858)
San Jose, CA 95125

3 John D. Tewhey
Lawrence Livermore Laboratory
P.O. Box 808
Livermore, CA 94550

J. G. Cline, General Manager
NYS ERDA
Agency Building #2
Empire State Plaza
Albany, NY 12233

Hayne Palmour, III
2140 Burlington Engineering Laboratories
North Carolina State University
Raleigh, NC 27607

J. P. Duckworth, Plant Manager
Nuclear Fuel Services, Inc.
P.O. Box 124
West Valley, NY 14171

E. H. Kobisk
Solid State Divison
Oak Ridge National Laboratory
Oak Ridge, TN 37830

No. of Copies

Oak Ridge National Laboratory
Central Research Library
Document Reference Section
P.O. Box X
Oak Ridge, TN 37830

A. L. Lotts
Oak Ridge National Laboratory
P.O. Box X
Oak Ridge, TN 37830

R. Roy
Pennsylvania State University
202 Materials Research Laboratory
University Park, PA 16802

2 A. B. Martin
Rockwell International
Energy Systems Group
8900 DeSoto Avenue
Canoga Park, CA 91304

R. G. Kepler
Organic and Electronic Department 5810
Sandia Laboratories
Albuquerque, NM 87185

2 N. J. Magnani
Sandia Laboratories
Division 5831
P.O. Box 5800
Albuquerque, NM 87185

M. A. Molecke
Sandia Laboratories
P.O. Box 5800
Albuquerque, NM 87185

M. D. Boersma
E. I. duPont deNemours and Company
Savannah River Laboratory
Aiken, SC 29801

No. of Copies

J. L. Crandall, Director
E. I. duPont deNemours and Company
Savannah River Laboratory
Aiken, SC 29801

3 R. G. Garvin
Savannah River Laboratory
P.O. Box A
Aiken, SC 29801

D. E. Gordon
E. I. duPont deNemours and Company
Savannah River Laboratory
Aiken, SC 29801

Jim Howel
E. I. duPont deNemours and Company
Savannah River Laboratory
Aiken, SC 29801

H. L. Hull
E. I. duPont deNemours and Company
Savannah River Laboratory
Aiken, SC 29801

A. S. Jennings
E. I. duPont deNemours and Company
Savannah River Laboratory
Aiken, SC 29801

J. A. Kelley
E. I. duPont deNemours and Company
Savannah River Laboratory
Aiken, SC 29801

R. Maher, Program Manager
Waste Management Programs
E. I. duPont deNemours and Company
Savannah River Laboratory
Aiken, SC 29801

No. of
Copies

D. L. McIntosh
E. I. duPont deNemours and Company
Savannah River Laboratory
Aiken, SC 29801

P. H. Permar
E. I. duPont deNemours and Company
Savannah River Laboratory
Aiken, SC 29801

S. Mirshak
E. I. duPont deNemours and Company
Savannah River Laboratory
Aiken, SC 29801

R. E. Blanco
Union Carbide Corporation (ORNL)
Chemical Technology Division
P.O. Box Y
Oak Ridge, TN 37830

J. O. Blomeke
Union Carbide Corporation (ORNL)
Chemical Technology Division
P.O. Box Y
Oak Ridge, TN 37830

D. E. Ferguson
Union Carbide Corporation (ORNL)
Chemical Technology Division
P.O. Box Y
Oak Ridge, TN 37830

H. W. Godbee
Union Carbide Corporation (ORNL)
Chemical Technology Division
P.O. Box Y
Oak Ridge, TN 37830

No. of
Copies

ONSITE

4 DOE Richland Operations Office

P. A. Craig
H. E. Ransom
M. W. Shupe
M. J. Zamorski

10 Rockwell Hanford Operations

W. J. Anderson (5)
E. L. Moore
M. J. Smith
D. D. Wodrich
B. J. Wood
File Copy

3 Westinghouse Hanford Company

A. G. Blasewitz
R. J. Cash
R. L. Fish

66 Pacific Northwest Laboratory

W. F. Bonner
D. J. Bradley
L. A. Charlot (15)
T. D. Chikalla
E. L. Courtright
S. D. Dahlgren
R. L. Dillon
R. P. Elmore
H. T. Fullam
C. R. Hann
A. J. Haverfield
J. H. Jarrett
M. R. Kreiter
W. L. Kuhn
L. T. Lakey
D. E. Larson
J. L. McElroy
M. D. Merz
J. E. Mendel
R. D. Nelson
R. E. Nightingale

No. of
Copies

S. G. Pitman
A. M. Platt
D. L. Prezbindowski
J. R. Serne
S. C. Slate
J. M. Rusin
R. T. Treat
R. P. Turcotte
R. E. Westerman (15)
G. E. Zima
Technical Information (5)
Publishing Coordination YO(2)